$(1 + 1)$-dimensional baryons from the SU(N) color-flavor transformation

J. Budczies [a], S. Nonnenmacher [b], Ya. Shnir [a], M.R. Zirnbauer [a]

[a] *Institut für Theoretische Physik, Universität zu Köln, 50937 Köln, Germany*
[b] *Service de Physique Théorique, CEA-Saclay, 91191 Gif-sur-Yvette Cedex, France*

Abstract

The color-flavor transformation, an identity that connects two integrals, each of which is over one of a dual pair of Lie groups acting in the fermionic Fock space, is extended to the case of the special unitary group. Using this extension, a toy model of lattice QCD is studied: N_f species of spinless fermions interacting with strongly coupled SU(N_c) lattice gauge fields in $1 + 1$ dimensions. The color-flavor transformed theory is expressed in terms of gauge singlets, the meson fields, organized into sectors distinguished by the distribution of baryonic flux. A comprehensive analytical and numerical search is made for saddle-point configurations of the meson fields, with various topological charges, in the vacuum and single-baryon sectors. Two definitions of the static baryon on the square lattice, straight and zigzag, are investigated. The masses of the baryonic states are estimated using the saddle-point approximation for large N_c. © 2002 Elsevier Science B.V. All rights reserved.

1. Introduction

In quantum chromodynamics (QCD), a hierarchy of scales is provided by $\Lambda_\chi \sim 1$ GeV, the scale of chiral symmetry breaking, and $\Lambda_{\text{QCD}} \sim 0.18$ GeV, defined as the location of the Landau pole of the one-loop beta function. The running coupling constant increases from weak to strong coupling as the momentum scale is lowered from the perturbative regime above Λ_χ down to Λ_{QCD}.

E-mail address: shnir@thp.uni-koeln.de (Ya. Shnir).

In the past two decades a great deal was learned about the non-perturbative structure of QCD at scales between Λ_χ and Λ_{QCD}. The guiding idea was to construct low-energy effective theories which encode the symmetries of the fundamental QCD Lagrangian. To obtain these effective theories, one may start from full QCD, and integrate out the high-energy degrees of freedom (quarks and gluons) in order to produce a low-energy effective action in terms of mesons and baryons. In this way it was possible to recover the chiral Lagrangian [1–4] that had been introduced phenomenologically by Weinberg [5].

In a more recent development, it was shown [6] how to extract the effective long-distance degrees of freedom by starting from the lattice [7,8] formulation of QCD. In that approach it is assumed that the long-distance physics of lattice QCD (LQCD) can be described by a strongly coupled lattice theory. From the latter, one gets the continuum chiral Lagrangian by expanding the effective action in powers of the lattice spacing and external momenta. All the terms of the Gasser–Leutwyler continuum effective Lagrangian [9] can be recovered in this way [10]. The lattice formulation is, however, deficient in one respect: by the technical difficulties with chiral symmetry for lattice fermions, the chiral anomaly is lost, i.e., for N_f massless quark flavors the chiral symmetry of the lattice effective theory is $\mathrm{U}(N_f)$ rather than $\mathrm{SU}(N_f)$.

This type of approach was initiated in [11,12]; it relied on a "bosonization" of the strong-coupling LQCD action, and a large-N_c or large-dimension expansion. Technically, the heart of the method is the computation of integrals over the group $\mathrm{SU}(N_c)$ with Haar measure, weighted by $\mathrm{e}^{-S(U)}$. Some general results for such integrals have recently been reviewed in [13].

A few years ago, an alternative kind of bosonization scheme was introduced [14], relying on a mathematical formalism later called the "color-flavor transformation" [15]. This transformation relates two different formulations of a certain class of theories. In condensed matter theory, the transformation has found a number of applications, among others to the random flux model [16].

The color-flavor transformation in its original version applies to the gauge group $\mathrm{U}(N_c)$. For this group, all gauge singlets are of "mesonic" (or quark–antiquark) type. In order for baryons to appear, one needs to replace $\mathrm{U}(N_c)$ by the special unitary group $\mathrm{SU}(N_c)$. In Section 2 of the present paper we extend the color-flavor transformation to $\mathrm{SU}(N_c)$, by decomposing the (colorless) flavor sector of Fock space into disconnected subsectors labeled by the baryonic charge.

In Sections 4–7 we apply the formalism to a toy model of LQCD: N_f species of spinless fermions interacting with strongly coupled $\mathrm{SU}(N_c)$ lattice gauge fields in $1+1$ dimensions. The color-flavor transformation yields a dual representation of this non-Abelian model. Combining numerical computations with analytical considerations, we conduct a comprehensive search for saddle-point configurations in various baryonic sectors with different topological properties. We use these configurations (without fluctuation corrections) to estimate the mass of a single baryon in our model. In doing so we ignore the Mermin–Wagner–Coleman theorem (asserting that spontaneous breaking of continuous global symmetries does not occur in $1+1$ dimensions), by assuming the pattern of chiral symmetry breaking that is known to occur in the physical case of $3+1$ dimensions.

After the present work had been completed, we learned that the $\mathrm{SU}(N)$ generalization of the color-flavor transformation has also been worked out by Schlittgen and Wettig [17].

2. Color-flavor transformation for SU(N_c)

2.1. Group action on fermionic Fock space

In this section we set up some algebraic structures, which are needed to establish the "color-flavor" transformation for the special unitary group. Our discussion follows the line of reasoning of Ref. [14] but is somewhat simpler, as we do not need the superalgebraic framework employed there.

We start by considering a set of fermionic creation and annihilation operators $\bar{f}_A^i$ and f_A^i, which obey the canonical anticommutation relations

$$\left\{ f_A^i, f_B^j \right\} = 0, \qquad \left\{ \bar{f}_A^i, \bar{f}_B^j \right\} = 0, \qquad \left\{ f_A^i, \bar{f}_B^j \right\} = \delta_{AB}\delta^{ij}.$$

The lower index takes the values $+a$ or $-a$, with range $a = 1, \dots, N_f$, and the upper index takes the values $i = 1, \dots, N_c$. Having QCD in mind, we interpret the operators $\bar{f}_{+a}^i$ and $\bar{f}_{-a}^i$ as creation operators for "quarks" and "antiquarks", respectively; the index i corresponds to the gauge (or color) degrees of freedom and the index a labels the different quark flavors. (The quarks are regarded here as being spinless.) The operators f_A^i and $\bar{f}_A^i$ act on a Fock space with vacuum $|0\rangle$ and its conjugate $\langle 0|$, by $f_A^i|0\rangle = 0$ and $\langle 0|\bar{f}_A^i = 0$ for all A and i.

We next consider the set of quadratic operators E_{AB}^{ij} defined by

$$E_{+a,+b}^{ij} = \bar{f}_{+a}^i f_{+b}^j, \qquad E_{+a,-b}^{ij} = \bar{f}_{+a}^i \bar{f}_{-b}^j,$$
$$E_{-a,+b}^{ij} = f_{-a}^i f_{+b}^j, \qquad E_{-a,-b}^{ij} = f_{-a}^i \bar{f}_{-b}^j.$$

The $\mathbb{C}$-linear span of these operators has the structure of a complex Lie algebra, $\mathfrak{G}$. More precisely, the operators E_{AB}^{ij} obey the commutation relations of a set of canonical generators of the Lie algebra $\mathfrak{gl}(2N_f N_c)$:

$$\left[E_{AB}^{ij}, E_{CD}^{kl} \right] = \delta^{jk}\delta_{BC} E_{AD}^{il} - \delta^{li}\delta_{DA} E_{CB}^{kj}.$$

Thus we have a Lie algebra isomorphism from $\mathfrak{gl}(2N_f N_c)$ (i.e., the space of complex matrices of size $2N_f N_c \times 2N_f N_c$, with the Lie bracket given by the commutator) to $\mathfrak{G}$:

$$t : \mathfrak{gl}(2N_f N_c) \to \mathfrak{G}, \qquad m \mapsto t_m := \sum_{ij, AB} m_{AB}^{ij} E_{AB}^{ij}.$$

This isomorphism lifts to an isomorphism of the corresponding complex groups:

$$T : \mathrm{GL}(2N_f N_c) \to G, \qquad M = \exp(m) \mapsto T_M = \exp(t_m), \tag{1}$$

which forms a (reducible) representation of $\mathrm{GL}(2N_f N_c)$ on Fock space. The representation is single-valued (which means there are no U(1) obstructions from the multi-valuedness of the logarithm) as the spectrum of each operator E_{AA}^{ii} is the set $\{0, 1\}$.

The Lie algebra $\mathfrak{gl}(2N_f N_c)$ has two subalgebras $\mathfrak{gl}(N_c)$ and $\mathfrak{gl}(2N_f)$ which are embedded in a natural way: a matrix $X \in \mathfrak{gl}(N_c)$ is identified with $I_{2N_f} \otimes X$, and a matrix $Y \in \mathfrak{gl}(2N_f)$ with $Y \otimes I_{N_c}$. Through these embeddings, $\mathfrak{gl}(N_c)$ and $\mathfrak{gl}(2N_f)$ form a pair of maximal commuting subalgebras of $\mathfrak{gl}(2N_f N_c)$, also known as a "dual pair" [18].

The subgroups $\mathrm{GL}(N_c)$ and $\mathrm{GL}(2N_f)$ are embedded into $\mathrm{GL}(2N_f N_c)$ in the same way. Their adjoint action on the fermionic creation and annihilation operators is described in Appendix A.

We define the *color group* to be the subgroup $\mathrm{SU}(N_c)$ of $\mathrm{GL}(N_c)$, and the *flavor group* to be the subgroup $\mathrm{U}(2N_f)$ of $\mathrm{GL}(2N_f)$. $\mathrm{GL}(N_c)$ contains an extra $\mathrm{U}(1)$ subgroup which lies outside the color group and, being generated by the unit matrix, commutes with the whole group $\mathrm{GL}(2N_f N_c)$. This $\mathrm{U}(1)$ is generated by $\widehat{Q} + N_f$ where

$$\widehat{Q} = \frac{1}{N_c} \sum_{A,i} E_{AA}^{ii} - N_f = \frac{1}{N_c} \sum_{a,i} (\bar{f}_{+a}^i f_{+a}^i - \bar{f}_{-a}^i f_{-a}^i) \tag{2}$$

counts the difference between the number of particles and the number of antiparticles: $\widehat{Q} = \frac{1}{N_c}(N_+ - N_-)$. In contrast, the operator giving the total number of particles, $\widehat{N} = \sum_{a,i}(\bar{f}_{+a}^i f_{+a}^i + \bar{f}_{-a}^i f_{-a}^i)$, does not commute with the generators of $\mathfrak{gl}(N_f)$. We will call $\widehat{Q}$ the *baryon charge operator*.

2.2. From color group integrals to flavor group integrals

Let ψ_A^i and $\bar{\psi}_A^i$ be two independent sets of Grassmann variables, referred to as "quark fields", and consider the color group integral

$$\mathcal{Z}(\psi, \bar{\psi}) = \int\limits_{\mathrm{SU}(N_c)} dU \, \exp\big(\bar{\psi}_{+a}^i U^{ij} \psi_{+a}^j + \bar{\psi}_{-b}^i \overline{U}^{ij} \psi_{-b}^j\big). \tag{3}$$

The Haar measure dU of $\mathrm{SU}(N_c)$ is understood to be normalized by $\int_{\mathrm{SU}(N_c)} dU = 1$. We also adopt the convention that repeated occurrence of an index implies summation.

The color-flavor transformation will replace the integral (3) by an integral over the flavor group $\mathrm{U}(2N_f)$. A key step in doing the transformation is to interpret $\mathcal{Z}(\psi, \bar{\psi})$ as the matrix element of an operator $\mathcal{P}$ that projects on the *colorless sector* (or flavor sector) of Fock space. This sector is the subspace of all states $|\text{flavor}\rangle$ which are invariant under the color group: $T_U|\text{flavor}\rangle = |\text{flavor}\rangle$ for all $U \in \mathrm{SU}(N_c)$.

The first step towards the color-flavor transformation is to express the projector $\mathcal{P}$ as

$$\mathcal{P} = \int\limits_{\mathrm{SU}(N_c)} dU \, T_U. \tag{4}$$

Let us now introduce the fermion coherent states

$$\langle \overline{\Psi}| = \langle 0| \exp\big(\bar{\psi}_{-a}^i f_{-a}^i + \bar{\psi}_{+a}^i f_{+a}^i\big), \qquad |\Psi\rangle = \exp\big(\bar{f}_{-a}^i \psi_{-a}^i + \bar{f}_{+a}^i \psi_{+a}^i\big)|0\rangle. \tag{5}$$

By making use of the first set of relations in Appendix A, it is straightforward to show that

$$\langle \overline{\Psi}|T_U|\Psi\rangle = \exp\big(\bar{\psi}_{+a}^i U^{ij} \psi_{+a}^j + \bar{\psi}_{-b}^i \overline{U}^{ij} \psi_{-b}^j\big)$$

for $U \in \mathrm{SU}(N_c)$. This yields the simple formula

$$\mathcal{Z}(\psi, \bar{\psi}) = \langle \bar{\Psi}|\mathcal{P}|\Psi\rangle. \tag{6}$$

To express $\mathcal{Z}(\psi, \bar{\psi})$ as an integral over the flavor group, we will derive an alternative representation of the projector $\mathcal{P}$, as an integral over coherent states of the flavor sector.

2.3. The flavor sector

The subspace of states in Fock space which are invariant under $U(N_c)$ was described in [14]. It consists of the vacuum and of *mesonic* excitations on top of it. The prototype of such an excitation is the "one-meson" state

$$|m_{ab}\rangle = \sum_i E^{ii}_{+a,-b}|0\rangle = \sum_i \bar{f}^i_{+a}\bar{f}^i_{-b}|0\rangle.$$

By the multiple action of the $\mathfrak{gl}(2N_f)$ generators $E^{ii}_{+a,-b}$ (where we have gone back to using the summation convention), one can build states containing up to $N_c N_f$ mesons, with different flavors. These states are automatically $U(N_c)$-invariant; conversely, all $U(N_c)$-invariant states are linear combinations of such multi-meson states. The group $U(2N_f)$ acts irreducibly on this invariant subspace.

The set of $SU(N_c)$-invariant states is larger. To obtain it, one relaxes the constraint $\widehat{Q}|\psi\rangle = 0$. Thus there exist colorless sectors of Fock space on which the central generator $\widehat{Q}$ takes a non-zero value. These sectors contain the *baryons*, which are totally antisymmetric combinations of N_c quarks. A baryon with flavors $a_1, \ldots, a_{N_c}$ is defined as

$$|b_{A_1 \ldots A_{N_c}}\rangle = \frac{1}{N_c!}\varepsilon_{i_1 \ldots i_{N_c}} \bar{f}^{i_1}_{A_1} \cdots \bar{f}^{i_{N_c}}_{A_{N_c}}|0\rangle, \tag{7}$$

where the $A_k = \pm a_k$ are taken either all positive (baryon), or all negative (antibaryon). A matrix $g \in GL(N_c)$ acts on this state simply by multiplication with $\text{Det}(g)$ (respectively, $\text{Det}^{-1}(g)$). Therefore, the state is invariant under the color group $SU(N_c)$.

The above baryon (respectively, antibaryon) is an eigenstate of the baryon charge operator $\widehat{Q}$ with eigenvalue $+1$ (respectively, -1). Acting on it with the generators E^{ii}_{AB} of the flavor algebra $\mathfrak{gl}(2N_f)$, one builds other colorless states with the same baryon number, which form an irreducible subspace for $U(2N_f)$: the one-baryon (respectively, one-antibaryon) sector.

The one-baryon sector can be generated from the state (7) with all $A_j = 1$. One can similarly build Q-baryon (respectively, Q-antibaryon) states from

$$|B_Q\rangle = \prod_{a=1}^{Q} \bar{f}^1_{+a} \cdots \bar{f}^{N_c}_{+a}|0\rangle, \qquad |B_0\rangle = |0\rangle, \qquad |B_{-Q}\rangle = \prod_{a=1}^{Q} \bar{f}^1_{-a} \cdots \bar{f}^{N_c}_{-a}|0\rangle. \tag{8}$$

The values of the baryon charge range from $-N_f$ to N_f, according to Pauli's exclusion principle. As with $Q = \pm 1$, acting on $|B_Q\rangle$ with the algebra $\mathfrak{gl}(2N_f)$ builds the full Q-baryon part of the flavor sector, so the group $U(2N_f)$ acts irreducibly on this part. This can be proved by using the dual-pair property of the subalgebras $\mathfrak{gl}(2N_f)$ and $\mathfrak{gl}(N_c)$, as exposed in [18].

To summarize, the flavor sector of Fock space decomposes into $2N_f + 1$ subsectors, characterized by their baryon charges Q. Each sector carries an irreducible unitary representation of the flavor group $U(2N_f)$.

2.4. Coherent states

Having decomposed the flavor sector as described above, we can now express the projector $\mathcal{P}$ in a different way. For this purpose we will use coherent states, in the spirit of Perelomov [19]. On each subsector with a fixed baryon charge Q, we consider the *generalized coherent states* built by the action of $G \equiv U(2N_f)$ on the reference state $|B_Q\rangle$, i.e., the states

$$\forall g \in G, \quad \forall Q = -N_f, \ldots, N_f: \quad |g_Q\rangle \overset{\text{def}}{=} T_g |B_Q\rangle, \qquad \langle g_Q| \overset{\text{def}}{=} \langle B_Q| T_g^\dagger. \tag{9}$$

The crucial property of coherent states we will now use, is that they supply a resolution of unity. Because of the irreducibility of the $U(2N_f)$ action on each Q-subsector, the operator

$$\mathcal{P}_Q \overset{\text{def}}{=} \alpha_Q \int\limits_G dg \, |g_Q\rangle\langle g_Q| \tag{10}$$

coincides with the orthogonal projector on that subsector, the only provision being that the normalization constant α_Q be chosen appropriately. Indeed, the operator $\mathcal{P}_Q$ trivially commutes with every element of the flavor group; Schur's lemma then ensures that it is proportional to the identity on each irreducible space of this group, therefore, on each subsector with fixed baryonic charge. Owing to orthogonality, $\mathcal{P}_Q$ vanishes on all subsectors with $Q' \neq Q$, whereas it is the identity on the Q-subsector if we take

$$\alpha_Q = \left(\int\limits_G dg \, |\langle B_Q| T_g |B_Q\rangle|^2 \right)^{-1}. \tag{11}$$

Some particular values of the constant (namely α_0, $\alpha_{\pm 1}$) are computed in Appendix B.

For the matrix element (6) of the projector $\mathcal{P}$ on the full flavor sector,

$$\mathcal{P} = \bigoplus_{Q=-N_f}^{N_f} \mathcal{P}_Q,$$

we now have a new representation:

$$\mathcal{Z}(\psi, \bar{\psi}) = \sum_{Q=-N_f}^{N_f} \alpha_Q \int\limits_G dg \, \langle \overline{\Psi}|g_Q\rangle\langle g_Q|\Psi\rangle. \tag{12}$$

To compute the overlaps $\langle \overline{\Psi}|g_Q\rangle$ and $\langle g_Q|\Psi\rangle$, it is convenient to use a Gauss decomposition of $G = U(2N_f)$: almost any matrix $g = \left(\begin{smallmatrix} A & B \\ C & D \end{smallmatrix} \right) \in G$ can be factored as

$$\begin{pmatrix} A & B \\ C & D \end{pmatrix} = \begin{pmatrix} 1 & Z \\ 0 & 1 \end{pmatrix} \begin{pmatrix} \tilde{A} & 0 \\ 0 & D \end{pmatrix} \begin{pmatrix} 1 & 0 \\ \tilde{Z} & 1 \end{pmatrix}, \tag{13}$$

where the relations $Z = BD^{-1}$, $\tilde{Z} = D^{-1}C$, and $\tilde{A} = A - BD^{-1}C$ hold. The decomposition becomes singular if D does, but this happens only on a submanifold of codimension one (and, hence, measure zero) of G. The unitarity of g implies $\tilde{Z} = -D^\dagger Z^\dagger A^{\dagger -1}$ and

allows to write the central matrix in the form

$$\begin{pmatrix} \tilde{A} & 0 \\ 0 & D \end{pmatrix} = \begin{pmatrix} (1 + ZZ^\dagger)^{1/2} & 0 \\ 0 & (1 + Z^\dagger Z)^{-1/2} \end{pmatrix} \begin{pmatrix} \mathcal{U} & 0 \\ 0 & \mathcal{V} \end{pmatrix}. \tag{14}$$

The matrices $\mathcal{U}$ and $\mathcal{V}$ are unitary, so $\begin{pmatrix} \mathcal{U} & 0 \\ 0 & \mathcal{V} \end{pmatrix}$ is an element of the diagonal $U(N_f) \times U(N_f)$ subgroup of G, which we call H. It can thus be shown that the elements g of an open dense subset of G are in one-to-one correspondence with the triplets $(Z, \mathcal{U}, \mathcal{V})$, where the pair $\mathrm{diag}(\mathcal{U}, \mathcal{V})$ is an element of H, while Z represents a point in the coset space G/H and can be any complex $N_f \times N_f$ matrix. Moreover, the Haar measure dg of G factorizes as

$$\int_G dg = \int_{G/H} d(gH) \int_H dh = \int_{\mathbb{C}^{N_f \times N_f}} d\mu(Z, Z^\dagger) \int_H d\mathcal{U} \, d\mathcal{V}. \tag{15}$$

Both $d\mathcal{U}$ and $d\mathcal{V}$ are normalized Haar measures on $U(N_f)$, and

$$d\mu(Z, Z^\dagger) = C_{N_f} \mathrm{Det}(1 + ZZ^\dagger)^{-2N_f} \prod_{i,j} dZ_{ij} \, d\overline{Z}_{ij}$$

is the normalized invariant measure on G/H. The normalization factor C_{N_f} is computed in Appendix B; see Eq. (B.6).

We now explain how to use this decomposition to compute the overlaps. The Gauss decomposition (13) carries over to any representation of G, so for every $g \in G$ we can write the operator T_g as

$$T_g = T_\zeta T_{\mathrm{diag}(\tilde{A}, D)} T_{\tilde{\zeta}}, \tag{16}$$

where $\zeta = \begin{pmatrix} 1 & Z \\ 0 & 1 \end{pmatrix}$ and $\tilde{\zeta} = \begin{pmatrix} 1 & 0 \\ \tilde{Z} & 1 \end{pmatrix}$. According to the relations given in Appendix A, the factors T_ζ and $T_{\tilde{\zeta}}$ act trivially on the reference states:

$$\forall Q = -N_f, \dots, N_f: \quad T_{\tilde{\zeta}} |B_Q\rangle = |B_Q\rangle, \qquad \langle B_Q| T_\zeta = \langle B_Q|. \tag{17}$$

The action of the block-diagonal operator is slightly more subtle. Using the third set of relations given in Appendix A, we get

$$T_{\mathrm{diag}(\tilde{A}, D)} |0\rangle = (\mathrm{Det}\, D)^{N_c} |0\rangle,$$

$$T_{\mathrm{diag}(\tilde{A}, D)} |B_1\rangle = (\mathrm{Det}\, D)^{N_c} \prod_{i=1}^{N_c} \tilde{A}_{a1} \bar{f}^i_{+a} |0\rangle,$$

$$T_{\mathrm{diag}(\tilde{A}, D)} |B_{-1}\rangle = (\mathrm{Det}\, D)^{N_c} \prod_{i=1}^{N_c} (D^{-1})_{1a} \bar{f}^i_{-a} |0\rangle.$$

(To make sense of these formulas one must remember that we are using the summation convention: the flavor index a under the product is understood to be summed over.) These formulas directly yield the desired overlaps with $\langle \overline{\Psi} |$:

$$\langle \overline{\Psi} | g_0 \rangle = (\mathrm{Det}\, D)^{N_c} \prod_{i=1}^{N_c} \exp(\bar{\psi}^i_{+a} Z_{ab} \bar{\psi}^i_{-b}),$$

$$\langle \overline{\Psi} | g_1 \rangle = (\text{Det } D)^{N_c} \prod_{i=1}^{N_c} \bar{\psi}_{+c}^i \tilde{A}_{c1} \exp\left(\bar{\psi}_{+a}^i Z_{ab} \bar{\psi}_{-b}^i\right),$$

$$\langle \overline{\Psi} | g_{-1} \rangle = (\text{Det } D)^{N_c} \prod_{i=1}^{N_c} D_{1c}^{-1} \bar{\psi}_{-c}^i \exp\left(\bar{\psi}_{+a}^i Z_{ab} \bar{\psi}_{-b}^i\right),$$

as well as the overlaps with $|\Psi\rangle$:

$$\langle g_0 | \Psi \rangle = \left(\text{Det } D^\dagger\right)^{N_c} \prod_{i=1}^{N_c} \exp\left(\psi_{-a}^i Z^\dagger{}_{ab} \psi_{+b}^i\right),$$

$$\langle g_1 | \Psi \rangle = \left(\text{Det } D^\dagger\right)^{N_c} \prod_{i=1}^{N_c} \tilde{A}_{1c}^\dagger \psi_{+c}^i \exp\left(\psi_{-a}^i Z^\dagger{}_{ab} \psi_{+b}^i\right),$$

$$\langle g_{-1} | \Psi \rangle = \left(\text{Det } D^\dagger\right)^{N_c} \prod_{i=1}^{N_c} \psi_{-c}^i \left(D^{-1}\right)_{c1}^\dagger \exp\left(\psi_{-a}^i Z^\dagger{}_{ab} \psi_{+b}^i\right).$$

The overlaps with the coherent states $|g_Q\rangle$ containing more than one baryon ($|Q| > 1$) can be computed in the same way; in front of the exponential factors, there will be $|Q|$ similar products, with flavor indices $1, \ldots, |Q|$.

We now insert the above expressions for the overlaps into (12), and use the factorization (15) to arrive at an integral over triples $(Z, \mathcal{U}, \mathcal{V})$. Leaving the Z-integral for later, we next carry out the integrations over the unitary matrices $\mathcal{U}$ and $\mathcal{V}$. They enter in the overlaps via the matrix elements of $\tilde{A}$ and D; see Eq. (14). To simplify the notation, we first perform a flavor rotation on the Grassmann fields:

$$\phi_{+b}^i = (\sqrt{1 + ZZ^\dagger})_{ba} \psi_{+a}^i, \qquad \phi_{-b}^i = \psi_{-a}^i (\sqrt{1 + Z^\dagger Z})_{ab},$$

$$\bar{\phi}_{+b}^i = \bar{\psi}_{+a}^i (\sqrt{1 + ZZ^\dagger})_{ab}, \qquad \bar{\phi}_{-b}^i = (\sqrt{1 + Z^\dagger Z})_{ba} \bar{\psi}_{-a}^i.$$

The integrals we need to compute then read as follows (assuming $Q > 0$):

$$\chi_Q(\bar{\phi}_+, \phi_+) \overset{\text{def}}{=} \alpha_Q \int_{\mathrm{U}(N_f)} d\mathcal{U} \prod_{c=1}^{Q} \prod_{i=1}^{N_c} \left(\bar{\phi}_{+a}^i \mathcal{U}_{ac}\right)\left(\phi_{+b}^i \mathcal{U}_{cb}^{-1}\right), \tag{18}$$

$$\chi_{-Q}(\bar{\phi}_-, \phi_-) \overset{\text{def}}{=} \alpha_{-Q} \int_{\mathrm{U}(N_f)} d\mathcal{V} \prod_{c=1}^{Q} \prod_{i=1}^{N_c} \left(\bar{\phi}_{-a}^i \mathcal{V}_{ca}^{-1}\right)\left(\phi_{-b}^i \mathcal{V}_{bc}\right). \tag{19}$$

We also set $\chi_0 \equiv \alpha_0$, and $\chi_Q(\bar{\psi}, \psi; Z) \equiv \chi_Q(\bar{\phi}_+, \phi_+)$, and $\chi_{-Q}(\bar{\psi}, \psi; Z) \equiv \chi_{-Q}(\bar{\phi}_-, \phi_-)$. The function $\chi_1(\bar{\phi}_+, \phi_+)$ will play a distinguished role in the lattice gauge theory application in Section 3, and we therefore evaluate it explicitly in the next subsection.

The integrations over H having been done, we are left with an integral over G/H, i.e., over a Z-dependent integrand, in each Q-subsector. Putting everything together, we finally arrive at the following identity:

$$\int\limits_{\mathrm{SU}(N_c)} dU \, \exp\big(\bar{\psi}^i_{+a} U^{ij} \psi^j_{+a} + \bar{\psi}^i_{-b} \overline{U}^{ij} \psi^j_{-b}\big)$$

$$= \sum_{Q=-N_f}^{N_f} \int\limits_{\mathbb{C}^{N_f \times N_f}} d\mu\big(Z, Z^\dagger\big) \chi_Q(\bar{\psi}, \psi; Z) \frac{\exp(\bar{\psi}^i_{+a} Z_{ab} \bar{\psi}^i_{-b} + \psi^j_{-b} Z^\dagger_{ba} \psi^j_{+a})}{\mathrm{Det}(1 + ZZ^\dagger)^{N_c}}, \tag{20}$$

which is called the color-flavor transformation for $\mathrm{SU}(N_c)$, and is the central result of the present section. Note that the right-hand side of the transformation has the attractive feature of organizing the contributions according to the different baryonic sectors.

An effective action in the bosonic variable Z can be obtained by doing the (Gaussian) integral over the Grassmann fields. This will be done in a lattice gauge context in Section 3.

2.5. Evaluation of χ_1

In this subsection we evaluate the coefficient

$$\chi_1(\bar{\phi}_+, \phi_+) = \alpha_1 \int\limits_{\mathrm{U}(N_f)} d\mathcal{U} \, \prod_{i=1}^{N_c} \big(\bar{\phi}^i_{+a} \mathcal{U}_{a1}\big)\big(\phi^i_{+b} \overline{\mathcal{U}}_{b1}\big).$$

Only the first column of the unitary matrix $\mathcal{U}$ occurs in the integrand, so the integral is effectively over a unit sphere in N_f-dimensional complex space, $\mathrm{S}^{2N_f-1} = \mathbb{C}^{N_f}/\mathbb{R}_+$. Parametrizing the latter by a complex vector $z = (z_1, \ldots, z_{N_f})$ with unit norm $|z| = 1$, we have

$$\chi_1(\bar{\phi}_+, \phi_+) = \alpha_1 \frac{\int_{|z|=1} d\Omega(z, \bar{z}) \prod_{i=1}^{N_c} (\bar{\phi}^i_{+a} z_a)(\phi^i_{+b} \bar{z}_b)}{\int_{|z|=1} d\Omega(z, \bar{z})},$$

where $d\Omega(z, \bar{z})$ is a $\mathrm{U}(N_f)$-invariant measure on the unit sphere $|z| = 1$. By homogeneity in z and $\bar{z}$, we may use the trick of replacing the numerator and denominator by integrals over $\mathbb{C}^{N_f}$, with a Gaussian weight function $\mathrm{e}^{-|z|^2}$ included in the integrands. The answer then easily follows from Wick's theorem:

$$\chi_1(\bar{\phi}_+, \phi_+) = \alpha_1 \frac{(N_f - 1)!}{(N_c + N_f - 1)!} \sum_{\sigma \in \mathfrak{S}_{N_c}} \mathrm{sgn}\, \sigma \prod_{i=1}^{N_c} \bar{\phi}^i_{+a} \phi^{\sigma(i)}_{+a}$$

$$= \alpha_1 \frac{(N_f - 1)!}{(N_c + N_f - 1)!} \sum_{\sigma \in \mathfrak{S}_{N_c}} \mathrm{sgn}\, \sigma \prod_{i=1}^{N_c} \bar{\psi}^i_{+a} \big(1 + ZZ^\dagger\big)_{ab} \psi^{\sigma(i)}_{+b}, \tag{21}$$

where $\mathfrak{S}_{N_c}$ denotes the group of permutations of the numbers $1, \ldots, N_c$.

This result was already obtained in [22]. More general considerations based on the group theoretical approach were presented in [17]. Our calculation of the pre-exponential factors $\chi_0, \chi_{\pm 1}$ are in agreement with the latter work where a general formula for χ_Q was derived.

3. Color-flavor transformation on the lattice

We consider a Euclidean $SU(N_c)$ gauge theory in $1 + d$ dimensions placed on a hypercubic lattice with lattice constant a. The fermions $\psi_b^i(n)$, with colors $i = 1, \ldots, N_c$ and flavors $b = 1, \ldots, N_f$, are put on lattice sites labeled by $n = (n_0, \ldots, n_d)$, while the gauge matrix variables $U(n + \frac{\hat{\mu}}{2}) = \exp[iag A_\mu(na + \frac{a\hat{\mu}}{2})] \in SU(N_c)$ are placed on lattice links $n + \hat{\mu}/2$ (we label links by their *middle points*), starting from sites n in any of the directions $\mu = 0, \ldots, d$. In the limit of a strong gauge coupling g, the gauge theory has the partition sum $\mathcal{Z} = \int \prod_n d\psi(n) d\bar{\psi}(n) \, \mathcal{Z}(\psi, \bar{\psi})$ with [11]

$$\mathcal{Z}(\psi, \bar{\psi}) = \prod_n e^{S_{m,\psi,\bar{\psi}}(n)} \prod_\mu \int_{SU(N_c)} dU\left(n + \frac{\hat{\mu}}{2}\right) \exp\left\{S_{U,\psi,\bar{\psi}}\left(n + \frac{\hat{\mu}}{2}\right)\right\}. \tag{22}$$

The fermions on two neighboring sites n and $n + \hat{\mu}$ are coupled through the gauge fields on the connecting link $n + \hat{\mu}/2$ in a gauge-invariant way:

$$S_{U,\psi,\bar{\psi}}\left(n + \frac{\hat{\mu}}{2}\right) = \frac{a^d}{2}\left[\bar{\psi}_b^i(n)U^{ij}\left(n + \frac{\hat{\mu}}{2}\right)\psi_b^j(n + \hat{\mu})\right.$$
$$\left. - \bar{\psi}_b^j(n + \hat{\mu})U^{\dagger ji}\left(n + \frac{\hat{\mu}}{2}\right)\psi_b^i(n)\right], \tag{23}$$

while the (bare) quark mass m couples the fermions diagonally

$$S_{m,\psi,\bar{\psi}}(n) = a^{d+1}m\bar{\psi}(n)\psi(n). \tag{24}$$

We are not going to worry here about the fermion doubling problem and will restrict our considerations to this naive discretization of the fermionic action. Also, for simplicity we do not take into account the spin degrees of freedom, leaving their inclusion for a future publication.

We rescale the fermionic fields so as to absorb the prefactor $a^d/2$. This just adds a global prefactor to $\mathcal{Z}$, and has no effect on the physical quantities. The $SU(N_c)$-integral over U on each link is then identical to (3) after the following substitutions:

$$\bar{\psi}_+ = \bar{\psi}(n), \qquad \psi_+ = \psi(n + \hat{\mu}), \qquad \bar{\psi}_- = \psi(n), \quad \psi_- = \bar{\psi}(n + \hat{\mu}).$$

On each link, we perform the color-flavor transformation (20), thereby introducing a complex "flavor matrix field" $Z(n + \frac{\hat{\mu}}{2})$, $Z^\dagger(n + \frac{\hat{\mu}}{2})$. The outcome of the transformation reads

$$\mathcal{Z}(\psi, \bar{\psi}) = \sum_{\{Q\}} \prod_n e^{2am\bar{\psi}(n)\psi(n)}$$
$$\times \prod_\mu \int_{\mathbb{C}^{N_f \times N_f}} d\mu\left(Z, Z^\dagger\left(n + \frac{\hat{\mu}}{2}\right)\right) \chi_{Z,\psi,\bar{\psi}}^Q\left(n + \frac{\hat{\mu}}{2}\right)$$
$$\times \frac{\exp\{S_{Z,\psi,\bar{\psi}}(n + \frac{\hat{\mu}}{2})\}}{\text{Det}(1 + Z^\dagger Z(n + \frac{\hat{\mu}}{2}))^{N_c}}, \tag{25}$$

where the sum on the right-hand side extends over all possible distributions $\{Q\}$ of baryonic charge (actually, baryonic flux) over the links of the lattice. The color-flavor transformed action on a link $n + \hat{\mu}/2$ is

$$S_{Z,\psi,\bar{\psi}}\left(n + \frac{\hat{\mu}}{2}\right) = \bar{\psi}_a^i(n) Z_{ab}\left(n + \frac{\hat{\mu}}{2}\right) \psi_b^i(n)$$
$$+ \bar{\psi}_b^j(n + \hat{\mu}) Z^\dagger{}_{ba}\left(n + \frac{\hat{\mu}}{2}\right) \psi_a^j(n + \hat{\mu}) , \qquad (26)$$

and the χ-coefficients are $\chi^0(n + \frac{\hat{\mu}}{2}) = \alpha_0$ and (with $Q = Q(n + \frac{\hat{\mu}}{2}) > 0$)

$$\chi_{Z,\psi,\bar{\psi}}^Q\left(n + \frac{\hat{\mu}}{2}\right)$$
$$= \chi_{Q(n+\frac{\hat{\mu}}{2})}\left(\bar{\psi}(n)\sqrt{1 + ZZ^\dagger\left(n + \frac{\hat{\mu}}{2}\right)}, \sqrt{1 + ZZ^\dagger\left(n + \frac{\hat{\mu}}{2}\right)}\psi(n + \hat{\mu})\right), \quad (27)$$

$$\chi_{Z,\psi,\bar{\psi}}^{-Q}\left(n + \frac{\hat{\mu}}{2}\right)$$
$$= \chi_{-Q(n+\frac{\hat{\mu}}{2})}\left(\sqrt{1 + Z^\dagger Z\left(n + \frac{\hat{\mu}}{2}\right)}\psi(n), \bar{\psi}(n + \hat{\mu})\sqrt{1 + Z^\dagger Z\left(n + \frac{\hat{\mu}}{2}\right)}\right). \quad (28)$$

The fermions are now coupled through their *flavor* indices, whereas in the original action the coupling had been mediated by the color degrees of freedom. Moreover, the coupling has become ultralocal: the fermions at a site n couple only to one another, via $Z(n + \frac{\hat{\mu}}{2})$, and so do the fermions at site $n + \hat{\mu}$, via $Z^\dagger(n + \frac{\hat{\mu}}{2})$. Correlations between neighbors are solely due to the relation between Z and $Z^\dagger$ by Hermitian conjugation. A graphical description of the change of coupling scheme is given in Fig. 1.

The partition function (25) is a sum over all configurations of baryonic fluxes $\{Q(n + \frac{\hat{\mu}}{2})\}$. For most of these configurations, the Grassmann integral vanishes identically. To see that, we expand the integrand for a given configuration into a polynomial in the Grassmann fields, and count (for each site n) the number of fermions $\psi(n)$, $\bar{\psi}(n)$ in the various monomials:
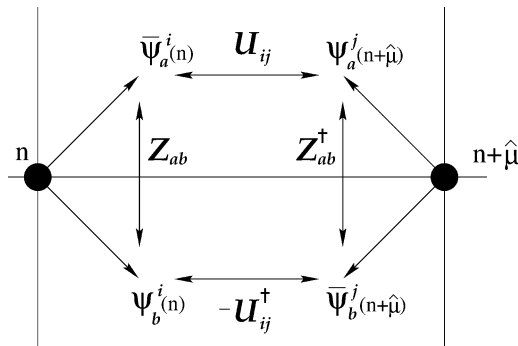

Fig. 1. Coupling of the fermion fields before and after the color-flavor transformation.

- For every direction μ, the coefficient $\chi^Q(n + \frac{\hat{\mu}}{2})$ contains $N_c|Q|$ Grassmann variables $\bar{\psi}_a^i(n)$ if $Q > 0$, and the same number of Grassmann variables $\psi_a^i(n)$ if $Q < 0$.
- For the coefficients $\chi^Q(n - \frac{\hat{\mu}}{2})$ the situation is the same, except that $\psi(n)$ and $\bar{\psi}(n)$ switch roles.
- Each term of the expansion of $e^{\bar{\psi}Z\psi + \bar{\psi}Z^\dagger\psi + 2am\bar{\psi}\psi}$ involves as many $\bar{\psi}(n)$ as $\psi(n)$.

The Grassmann integral $\int d\psi(n)\, d\bar{\psi}(n)$ extracts the coefficient of the top-monomial,

$$\int d\bar{\psi}(n)\, d\psi(n) \prod_{i=1}^{N_c} \prod_{a=1}^{N_f} \psi_a^i(n)\bar{\psi}_a^i(n) = 1,$$

setting all others to zero. This monomial contains as many $\bar{\psi}(n)$ as $\psi(n)$. Hence, in view of the counting above, the contribution from a configuration $\{Q(n + \frac{\hat{\mu}}{2})\}$ vanishes unless the following condition is met:

$$\sum_{\mu=0}^{d} Q\left(n + \frac{\hat{\mu}}{2}\right) = \sum_{\mu=0}^{d} Q\left(n - \frac{\hat{\mu}}{2}\right). \tag{29}$$

The physical meaning of this equation is conservation of the baryon current: the (algebraic) number of baryons "arriving" at the site n (from the links $n - \hat{\mu}/2$) must equal the number of baryons "leaving" the site (via the links $n + \hat{\mu}/2$).

The general structure of the partition function (25) corresponds to the hadronic correlation function written in terms of colorless N_c-quark currents [20,21].

3.1. Integration over the fermions

Based on the general considerations above, we perform the integration over the fermions sector by sector, and present below two particular cases: the "vacuum", i.e., the sector where the baryonic flux $Q(n + \frac{\hat{\mu}}{2})$ vanishes on every link $n + \hat{\mu}/2$, and a toy model of a static baryon on a mesonic background (with $Q(n + \frac{\hat{\mu}}{2}) = 1$ along a time axis).

In each case, integration over the Grassmann variables yields a purely bosonic effective action, which depends on the configuration of the fields Z and $Z^\dagger$. After computing these effective actions, we will look for their saddle-point configurations to estimate the respective partition functions.

Before computing the effective actions in particular cases, we emphasize the consequences of chiral symmetry, which emerges in the limit of zero quark mass. The hypercubic lattice is bipartite, so it can be split into two sublattices according to the parity of $|n| \overset{\text{def}}{=} \sum_\mu n_\mu$. Given this splitting, the effective actions $S(Z, Z^\dagger)$ of all sectors are invariant under the following global transformation:

$$|n|\ \text{even:} \quad Z\left(n + \frac{\hat{\mu}}{2}\right) \mapsto U_1 Z\left(n + \frac{\hat{\mu}}{2}\right) U_2,$$

$$Z^\dagger\left(n + \frac{\hat{\mu}}{2}\right) \mapsto U_2^\dagger Z^\dagger\left(n + \frac{\hat{\mu}}{2}\right) U_1^\dagger,$$

$$|n| \text{ odd:} \quad Z\left(n + \frac{\hat{\mu}}{2}\right) \mapsto U_2^\dagger Z\left(n + \frac{\hat{\mu}}{2}\right) U_1^\dagger,$$

$$Z^\dagger\left(n + \frac{\hat{\mu}}{2}\right) \mapsto U_1 Z^\dagger\left(n + \frac{\hat{\mu}}{2}\right) U_2, \tag{30}$$

for any pair $(U_1, U_2) \in \mathrm{U}(N_f) \times \mathrm{U}(N_f)$. Therefore, in each sector, the saddle-point configurations in the chiral limit form a continuous set (namely an "orbit") generated by acting with the chiral symmetry group $\mathrm{U}(N_f) \times \mathrm{U}(N_f)$. As soon as the quark masses are turned on, this degeneracy disappears, and the saddle points become isolated. Eq. (30) show that the fields Z, $Z^\dagger(n + \frac{\hat{\mu}}{2})$ transform differently according to the parity of $|n|$. To stress this difference, we give different names to the fields on different sublattices: the fields living on the "even" lattice links will be called V, $V^\dagger(n + \frac{\hat{\mu}}{2})$, while the fields on the "odd" links will be denoted by W, $W^\dagger(n + \frac{\hat{\mu}}{2})$.

3.1.1. Vacuum action

For the vacuum sector we have zero baryonic flux ($Q = 0$) everywhere on the lattice; the integral over the fermions, being Gaussian, is then easily done and yields

$$\mathcal{Z}_{\text{vacuum}} = \int d\bar{\psi}(n)\, d\psi(n)\, \mathcal{Z}_{\text{vacuum}}(\psi, \bar{\psi})$$

$$= \int \left\{ \prod_{n,\mu} \alpha_0\, d\mu\left(Z, Z^\dagger\left(n + \frac{\hat{\mu}}{2}\right)\right) \right\} \exp(-N_c S_{\text{vacuum}}[Z]), \tag{31}$$

where the result of the integration has been sent back to the exponent. The integration measure in curly brackets will be denoted by $\mathcal{D}(Z, Z^\dagger)$ in the following. The factor N_c in the exponent comes from the color content of the fermions: since the action $S_Z(\bar{\psi}, \psi)$ does not couple fermions with different colors, the Grassmann integral is a product of N_c identical integrals. The effective action is

$$S_{\text{vacuum}} = -\sum_n \mathrm{Tr} \ln M(n) + \sum_n \sum_{\mu=0}^d \mathrm{Tr} \ln N\left(n + \frac{\hat{\mu}}{2}\right), \tag{32}$$

where

$$M(n) \stackrel{\text{def}}{=} 2am + \sum_{\mu=0}^d \left[Z\left(n + \frac{\hat{\mu}}{2}\right) + Z^\dagger\left(n + \frac{\hat{\mu}}{2}\right) \right], \tag{33}$$

$$N\left(n + \frac{\hat{\mu}}{2}\right) \stackrel{\text{def}}{=} 1 + Z\left(n + \frac{\hat{\mu}}{2}\right) Z^\dagger\left(n + \frac{\hat{\mu}}{2}\right). \tag{34}$$

3.1.2. Static baryon action

By the static baryon we mean the following distribution of baryonic fluxes over the lattice: $Q(n + \frac{\hat{\mu}}{2}) = 1$ along the links of the "world line" (or "string") $n = (t, 0, \ldots, 0) \in \mathbb{Z}^{1+d}$, $\hat{\mu} = \hat{0}$, with $t = 0, \ldots, T - 1$; on all other links $Q = 0$ (see Fig. 2). This distribution satisfies the current conservation law (29) at all sites but the ends $t = 0$ and $t = T$
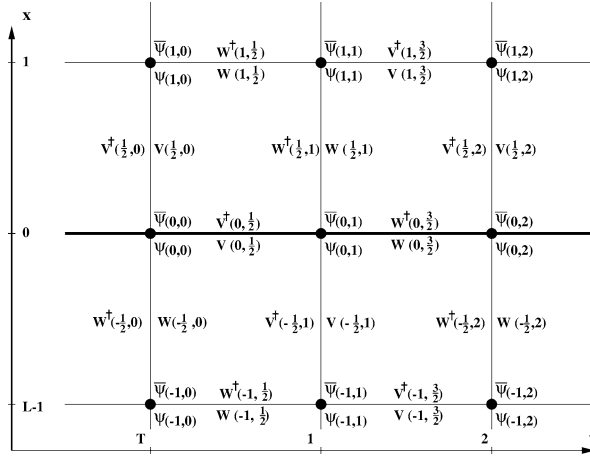
Fig. 2. Baryon string placed on a two-dimensional lattice.

of the world line. There it does, too, if we impose periodic (or antiperiodic) boundary conditions on the Grassmann fields: for a lattice of size T in the time direction, we set $\psi(T+1, \vec{r}) = \psi(1, \vec{r})$, $\bar{\psi}(T+1, \vec{r}) = \bar{\psi}(1, \vec{r})$. We again write the partition function in the form (31),

$$\mathcal{Z}_{\text{baryon}} = \int \mathcal{D}\bar{\psi}\, \mathcal{D}\psi\, \mathcal{Z}_{\text{baryon}}(\psi, \bar{\psi}) = \int \mathcal{D}(Z, Z^{\dagger}) \exp(-N_c S_{\text{baryon}}[Z]). \tag{35}$$

The effective action S_{baryon} contains the "sea" term $S_{\text{vacuum}}[Z]$, plus an extra part coming from the factors χ_1 along the world line of the baryon. These factors depend on the values of the Z field along this line and on the adjacent links, through the following matrix:

$$\mathsf{G} \overset{\text{def}}{=} N\left(\frac{1}{2}\hat{0}\right) M(1\hat{0})^{-1} N\left(\frac{3}{2}\hat{0}\right) \cdots N\left(\left(T - \frac{3}{2}\right)\hat{0}\right)$$
$$\times M((T-1)\hat{0})^{-1} N\left(\left(T - \frac{1}{2}\right)\hat{0}\right) M(T\hat{0})^{-1}. \tag{36}$$

(We use the abbreviation $t\hat{0} \equiv 0 + t\hat{0}$ to denote the sites or links on the world line of the baryon.) This product of matrices runs over all sites n on the baryon world line (it is expressed as a "quark propagator" along that line). In Appendix C we show that the effective action takes the form

$$e^{-N_c S_{\text{baryon}}[Z]} = \frac{1}{N_c!} \left\{ \frac{\alpha_0}{\alpha_1} \binom{N_c + N_f - 1}{N_c} \right\}^{-T}$$
$$\times \sum_{\hat{\sigma} \in \hat{\mathfrak{S}}_{N_c}} \mathcal{N}(\hat{\sigma}) \prod_{l=1}^{N_c} (\text{Tr}\,\mathsf{G}^l)^{c_l(\hat{\sigma})} e^{-N_c S_{\text{vacuum}}[Z]}. \tag{37}$$

In the non-vacuum factor of (37), $\hat{\sigma}$ runs over all conjugacy classes of the group $\mathfrak{S}_{N_c}$ of permutations of the set $\{1, \ldots, N_c\}$. Every representative of the class $\hat{\sigma}$ can be decomposed

as a product of cycles of various lengths l, such that $c_l(\hat{\sigma})$ cycles of length l occur; thus, each class $\hat{\sigma}$ is uniquely specified by the sequence $\{c_l\}$, or equivalently by a Young diagram. The weight factor $\mathcal{N}(\hat{\sigma})$ is simply the cardinality of the class $\hat{\sigma}$, and is given by

$$\mathcal{N}(\hat{\sigma}) = \frac{N_c!}{\prod_{l=1}^{N_c} l^{c_l(\hat{\sigma})} c_l(\hat{\sigma})!}. \tag{38}$$

For the lowest numbers of colors the explicit expressions are

$$N_c = 1: \quad S_{\text{baryon}} = S_{\text{vacuum}} - \ln \text{Tr}\, \mathsf{G} + \text{const},$$

$$N_c = 2: \quad S_{\text{baryon}} = S_{\text{vacuum}} - \frac{1}{2} \ln\big((\text{Tr}\,\mathsf{G})^2 + \text{Tr}\,\mathsf{G}^2\big) + \text{const},$$

$$N_c = 3: \quad S_{\text{baryon}} = S_{\text{vacuum}} - \frac{1}{3} \ln\big((\text{Tr}\,\mathsf{G})^3 + 3\,\text{Tr}\,\mathsf{G}^2\,\text{Tr}\,\mathsf{G} + 2\,\text{Tr}\,\mathsf{G}^3\big) + \text{const}. \tag{39}$$

The constants, which are not given above, make contributions to the baryon mass, so they need to be taken into account in the final answer.

In the following section, we look for the saddle-point configurations of the effective actions S_{vacuum} and S_{baryon}.

3.2. Saddle-point equations

In the two sectors that we are interested in—the vacuum and the static baryon—we wish to compute, or at least estimate, the partition functions (31), respectively, (35). Since we are unable to provide an exact answer, we will treat both integrals in a saddle-point approximation, valid in the limit of a large number of colors N_c. For both the vacuum and the static baryon, we will restrict ourselves to a purely classical approximation, which is to say we will identify the saddle points, evaluate the action functional on them, and approximate the partition function as $\mathcal{Z} \sim e^{-S(Z_{\text{s.p.}})}$. Thus we neglect all loop corrections, which are of higher order in $1/N_c$.

In the vacuum sector, where N_c appears explicitly as a factor of $S_{\text{vacuum}}[Z]$, the saddle-point approximation is fully justified in the large-N_c limit. The situation is less transparent in the static-baryon sector (37). However, for the ansatz made below, the matrix G is proportional to unity: $\mathsf{G} = \mathsf{g}\mathbb{I}_{N_f}$. (Note that G transforms under the chiral transformation (30) as $\mathsf{G} \mapsto U\mathsf{G}U^{-1}$, so the multiples of unity are fixed points of this group action.) If one decides to consider only those configurations of Z and $Z^{\dagger}$ for which G is scalar, the static-baryon action (37) simplifies to

$$S_{\text{baryon}}[Z] = S_{\text{vacuum}}[Z] - \log \mathsf{g} + \text{const},$$

so the saddle-point expansion is rigorously justified (for large N_c) if the integral is restricted to these configurations. We will use it to approximate the full integral.

4. Vacuum saddle-point configurations

The saddle-point analysis for the action functional $S_{\text{vacuum}}[Z]$ has already been carried out in [16,22,23], so we are going to be brief here. In varying the action (32), the complex

matrices Z and $Z^\dagger$ are to be considered as independent, which leads to two sets of equations. Variations of $Z(n + \frac{\hat{\mu}}{2})$ affect only the blocks $M(n)$ and $N(n + \frac{\hat{\mu}}{2})$, with the linear response being

$$\delta S_{\text{vacuum}} = \text{Tr}\left(-M(n)^{-1} + Z^\dagger\left(n + \frac{\hat{\mu}}{2}\right)N\left(n + \frac{\hat{\mu}}{2}\right)^{-1}\right)\delta Z\left(n + \frac{\hat{\mu}}{2}\right).$$

The resulting saddle-point equation reads $M(n)^{-1} = Z^\dagger(n + \frac{\hat{\mu}}{2})N(n + \frac{\hat{\mu}}{2})^{-1}$ or, by taking the inverse on both sides,

$$M(n) = Z\left(n + \frac{\hat{\mu}}{2}\right) + Z^\dagger\left(n + \frac{\hat{\mu}}{2}\right)^{-1}. \tag{40}$$

Similarly, the variation $\delta Z^\dagger(n - \frac{\hat{\nu}}{2})$ influences $M(n)$ and $N(n - \frac{\hat{\nu}}{2})$, and yields the saddle-point equation $M(n)^{-1} = N(n - \frac{\hat{\nu}}{2})^{-1}Z(n - \frac{\hat{\nu}}{2})$, which is equivalent to

$$M(n) = Z^\dagger\left(n - \frac{\hat{\nu}}{2}\right) + Z\left(n - \frac{\hat{\nu}}{2}\right)^{-1}. \tag{41}$$

As an immediate corollary, we have

$$Z\left(n + \frac{\hat{\mu}}{2}\right) + Z^\dagger\left(n + \frac{\hat{\mu}}{2}\right)^{-1} = Z^\dagger\left(n - \frac{\hat{\nu}}{2}\right) + Z\left(n - \frac{\hat{\nu}}{2}\right)^{-1} \tag{42}$$

at every site n and for any pair μ, ν.

4.1. Homogeneous vacuum

The simplest possibility for the field Z, $Z^\dagger$ is the scalar ansatz $Z = Z^\dagger = z\mathbb{I}$, with z a spacetime-independent real number. The vacuum saddle-point Eqs. (40) and (41) are solved by this ansatz if we put

$$z = z_\pm = \pm\frac{1}{\sqrt{2d+1}}\sqrt{1 + \frac{(am)^2}{2d+1}} - \frac{am}{2d+1}. \tag{43}$$

If $m > 0$, the action S_{vacuum} takes different values on these solutions. Expanding it in powers of (am), we get

$$S_{\text{vacuum}}[z_\pm] = L^{d+1}N_f\left[\ln\left(\frac{(2d+2)^d}{(2d+1)^{d+1/2}}\right) \mp \frac{\sqrt{2d+1}}{d+1}am\right], \tag{44}$$

which shows that for a positive quark mass, the configuration $z \equiv z_+$ minimizes the action.

In the chiral limit ($m = 0$), a continuous set of solutions is obtained by applying the transformations (30) to the homogeneous configuration $Z = Z^\dagger = z_{\text{vac}}\mathbb{I}$ for

$$z_{\text{vac}} = (2d + 1)^{-1/2}.$$

This vacuum configuration is invariant under the transformations of the diagonal subgroup $U_1 = U_2 \in U(N_f)$ of the chiral symmetry group, but it maps to a new "vacuum"

by taking $U_1 = U \in \mathrm{U}(N_f)$, $U_2 = \mathbb{I}_{N_f}$. By the Goldstone mechanism, the breaking of the continuous $\mathrm{U}(N_f)$ symmetry leads to the existence of massless modes, namely the mesons, an effective Lagrangian for which was obtained by expanding S_{vacuum} near this vacuum in [16,22].

If $\pm \mathbb{I} \neq U \in \mathrm{U}(N_f)$, the vacua obtained by translating the homogeneous one by U are staggered, in the sense that the value of Z depends on the parity of its position. However, on adopting the notations $V(n + \frac{\hat{\mu}}{2})$, $W(n' + \frac{\hat{\mu}}{2})$ for fields on the even and odd sublattices, the staggered vacua become homogeneous for each sublattice:

$$V\left(n + \frac{\hat{\mu}}{2}\right) = (2d + 1)^{-1/2} U, \qquad W\left(n' + \frac{\hat{\mu}}{2}\right) = (2d + 1)^{-1/2} U^\dagger. \tag{45}$$

In [23], it was proved that, modulo the $\mathrm{U}(N_f)$ degeneracy, the configuration $Z \equiv z_{\mathrm{vac}}$ is the *unique* solution of the vacuum saddle-point equations in the chiral limit (except in dimension $d = 0$, where the symmetry of the action is larger). The proof proceeds by a local argument, showing that for each site n the $2(d + 1)$ saddle-point equations involving $M(n)$ imply the equality of the matrices $Z(n + \frac{\hat{\mu}}{2})$, $Z^\dagger(n + \frac{\hat{\mu}}{2})$ for all $\mu = 0, \ldots, d$; iteration of this result then trivially leads to the set of staggered configurations (45). The proof strongly relies on $Z^\dagger$ being the Hermitian conjugate of Z, a constraint which is not mandatory. By relaxing it, we are now going to find a plethora of additional solutions of the vacuum saddle-point equations.

4.2. Nonhomogeneous vacuum configurations

By *local* considerations, as stated above, the only solutions of the vacuum saddle-point equations (and the Hermiticity constraint relating Z to $Z^\dagger$) in the chiral case are homogeneous in both sublattice fields V and W. However, on a finite lattice, say with the topology of a $(d + 1)$-dimensional torus $L^d \times T$, there is also a *global* aspect to consider: one has to make a choice of boundary conditions for the various fields. The simplest choice are periodic boundary conditions in all directions, but one can also impose θ-twisted boundary conditions, say along the first spatial direction $\hat{1}$:

$$V\left(n + \frac{\hat{\mu}}{2} + L\hat{1}\right) = e^{i\theta} V\left(n + \frac{\hat{\mu}}{2}\right),$$
$$W\left(n' + \frac{\hat{\mu}}{2} + L\hat{1}\right) = e^{-i\theta} W\left(n' + \frac{\hat{\mu}}{2}\right), \tag{46}$$

for all n and $\hat{\mu}$. An opposite twist for the fields V, W is natural in view of their opposite behavior under the chiral transformations (30).

Now, accepting these twisted boundary conditions, let us investigate which configuration will minimize the action (32). A homogeneous configuration suffers from a "phase jump" along a d-dimensional boundary, which is energetically very costly. A more reasonable ansatz for a minimum of the action is the following: the fields V, W smoothly rotate their phase, starting from V, $W \approx z_{\mathrm{vac}}$ for $n_1 = 1$, to $V = e^{i\theta} z_{\mathrm{vac}}$, $W = e^{-i\theta} z_{\mathrm{vac}}$ at $n_1 = L$, with a linear phase evolution in between. In this way, everywhere in spacetime the configuration *locally* looks like one of the degenerate homogeneous vacua.

4.2.1. Contour deformation

The above ansatz for V, W is only qualitative. In order to actually obtain field configurations that satisfy *both* the twisted boundary conditions (46) *and* the saddle-point equations (40), (41), we need to relax the Hermiticity relation between the fields Z and $Z^\dagger$.

By its construction via the color-flavor transformation, the integrand $\mathrm{e}^{-S_{\mathrm{vacuum}}}$ is to be viewed primarily as a function of the *real* variables $\{(Z_{ab} + Z_{ba}^\dagger)(n + \frac{\hat{\mu}}{2}),\ \mathrm{i}(Z_{ab} - Z_{ba}^\dagger)(n + \frac{\hat{\mu}}{2})\}$, the total number of which is $D = 2N_f^2\,(d+1)\,(TL^d)$. From [23], this function for $\theta \notin 2\pi\mathbb{Z}$ has no saddle points on $\mathbb{R}^D$, but it can be analytically continued into $\mathbb{C}^D$, where *complex saddle points* may exist. On such a saddle point there must exist at least one link $(n + \frac{\hat{\mu}}{2})$ where the matrix $Z^\dagger$ differs from the Hermitian conjugate of Z.

If a complex saddle point is not "too far" from the original contour of integration, it contributes to the vacuum-sector partition function, upon deforming the contour of integration so as to reach that point.

4.2.2. Vacuum saddle-point equations for twisted fields

We will demonstrate below the existence of complex saddle points for the vacuum sector with any θ-twist. To make things simpler, we restrict ourselves to a 2-dimensional spacetime, with a twist in the spatial boundary conditions (we call the time index t, the spatial index x). The above qualitative ansatz for the fields V, W suggests the following symmetries:

- All fields are scalar, i.e., at each point Z and $Z^\dagger$ are multiples of the identity matrix.
- The fields V, W are time-independent. For each position x, there are 4 field variables associated with the time-like link which we denote by $v_0(x)$, $w_0(x)$, $v_0^*(x)$, $w_0^*(x)$, and 4 field variables associated with the space direction, which we denote by $v_1(x + 1/2)$, $w_1(x + 1/2)$, $v_1^*(x + 1/2)$, $w_1^*(x + 1/2)$.

Thus, at each position $x = 0, \ldots, L - 1$ we have 8 independent complex variables. In the chiral limit ($m = 0$), the saddle-point equation (40) pertaining to $M(x, t)$ on an even site (x, t) read

$$
\begin{aligned}
& v_0(x) + w_0^*(x) + v_1(x + 1/2) + w_1^*(x - 1/2) \\
&= v_0(x) + 1/v_0^*(x) \\
&= w_0^*(x) + 1/w_0(x) \\
&= v_1(x + 1/2) + 1/v_1^*(x + 1/2) \\
&= w_1^*(x - 1/2) + 1/w_1(x - 1/2).
\end{aligned}
\tag{47}
$$

Eq. (41) pertaining to $M(x, t + 1)$ are obtained by interchanging $v \leftrightarrow w$, $v^* \leftrightarrow w^*$. For a finite quark mass, $2am$ is to be added to the left-hand side.

- The two first equations, together with their $v \leftrightarrow w$ exchange analogs, allow us one more simplification. Indeed, they imply the identities $v_0(x) = w_0^*(x)$, $v_0^*(x) = w_0(x)$ (the alternative possibility, $v_0(x) = 1/w_0(x)$ and $v_0^*(x) = 1/w_0^*(x)$, is incompatible

with other relations that need to be satisfied). So there remain only 6 complex variables for each x.

In the next section, we will provide approximate solutions for Eq. (47) together with their $v \leftrightarrow w$ partners and assuming the above symmetries.

4.2.3. Linearized problem

To solve (at least approximately) the above equations, we will use the fact that we expect the fields to be locally close to one of the configurations (45). We can then expand the saddle-point equations to first order in the perturbations from that configuration, and solve the linear problem. We start by expanding the fields around the real positive vacuum $V, W = \mathbb{I}/\sqrt{3}$:

$$v_0(x) = \frac{1}{\sqrt{3}}\big(1 + \delta v_0(x)\big),$$

$$v_0^*(x) = \frac{1}{\sqrt{3}}\big(1 + \delta v_0^*(x)\big),$$

$$v_1(x + 1/2) = \frac{1}{\sqrt{3}}\big(1 + \delta v_1(x + 1/2)\big),$$

$$v_1^*(x + 1/2) = \frac{1}{\sqrt{3}}\big(1 + \delta v_1^*(x + 1/2)\big),$$

$$w_1(x + 1/2) = \frac{1}{\sqrt{3}}\big(1 + \delta w_1(x + 1/2)\big),$$

$$w_1^*(x + 1/2) = \frac{1}{\sqrt{3}}\big(1 + \delta w_1^*(x + 1/2)\big).$$

After inserting these expressions into (47) and expanding to linear order, we obtain a "transfer matrix representation" of these equations, i.e., a linear equation relating the vector of deviations of the spatial components of the fields $\{\delta v_1, \delta v_1^*, \delta w_1, \delta w_1^*\}$ at position $x + 1/2$, to the same vector at position $x - 1/2$. The structure of the 4×4 transfer matrix allows to decompose it into two 2×2 matrices, upon considering at each point the vectors

$$\mathsf{R} = \begin{pmatrix} \delta v_1 + \delta w_1 \\ \delta v_1^* + \delta w_1^* \end{pmatrix}, \qquad \mathsf{I} = \begin{pmatrix} \delta v_1 - \delta w_1 \\ \delta v_1^* - \delta w_1^* \end{pmatrix}. \tag{48}$$

In terms of these two vectors, the linearized equations read

$$\mathsf{R}(x + 1/2) = \begin{pmatrix} -6 & 1 \\ -1 & 0 \end{pmatrix} \mathsf{R}(x - 1/2) \overset{\text{def}}{=} \mathsf{T}_r \mathsf{R}(x - 1/2), \tag{49}$$

$$\mathsf{I}(x + 1/2) = \begin{pmatrix} 3/2 & -1/2 \\ 1/2 & 1/2 \end{pmatrix} \mathsf{I}(x - 1/2) \overset{\text{def}}{=} \mathsf{T}_i \mathsf{I}(x - 1/2). \tag{50}$$

Similarly, the deviations of the temporal components $\delta v_0(x)$, $\delta v_0^*(x)$ are determined by the variations at $x - 1/2$:

$$\begin{pmatrix} \delta v_0(x) \\ \delta v_0^*(x) \end{pmatrix} = \begin{pmatrix} 3/4 & -1/4 \\ 3/4 & -1/4 \end{pmatrix} \mathsf{R}(x - 1/2) + \begin{pmatrix} 3/8 & -1/8 \\ -3/8 & 1/8 \end{pmatrix} \mathsf{I}(x - 1/2). \tag{51}$$

Thus, the transfer matrix allows to express the linear variation of all fields by the deviations at position $1/2$.

To make the x-dependence more explicit, we seek to diagonalize the transfer matrices T_r and T_i. The first transfer matrix T_r has the eigenvalues

$$-\mathrm{e}^{\pm\lambda} \overset{\mathrm{def}}{=} -(3 \pm 2\sqrt{2}), \quad \text{associated to the vectors } \mathsf{R}_\pm \overset{\mathrm{def}}{=} \begin{pmatrix} 1 \\ \mathrm{e}^{\mp\lambda} \end{pmatrix}. \tag{52}$$

The second transfer matrix T_i cannot be diagonalized but only put in Jordan normal form. Indeed, it acts on the vectors

$$\mathsf{I}_+ \overset{\mathrm{def}}{=} \begin{pmatrix} 1 \\ 1 \end{pmatrix}, \qquad \mathsf{I}_- \overset{\mathrm{def}}{=} \begin{pmatrix} 1 \\ -1 \end{pmatrix} \tag{53}$$

as

$$\mathsf{T}_i\,\mathsf{I}_+ = \mathsf{I}_+ + \mathsf{I}_-, \qquad \mathsf{T}_i\,\mathsf{I}_- = \mathsf{I}_-.$$

Therefore, an initial deviation

$$\mathsf{R}(1/2) = c_{+r}\,\mathsf{R}_+ + c_{-r}\,\mathsf{R}_-, \qquad \mathsf{I}(1/2) = c_{+i}\,\mathsf{I}_+ + c_{-i}\,\mathsf{I}_-$$

propagates through the transfer matrix as follows:

$$\begin{aligned}
\mathsf{R}(x+1/2) &= c_{+r}\left(-\mathrm{e}^\lambda\right)^x \mathsf{R}_+ + c_{-r}\left(-\mathrm{e}^{-\lambda}\right)^x \mathsf{R}_-, \\
\mathsf{I}(x+1/2) &= c_{+i}\,\mathsf{I}_+ + (c_{-i} + x c_{+i})\,\mathsf{I}_-.
\end{aligned} \tag{54}$$

This linear evolution is only valid as long as the deviations from $1/\sqrt{3}$ are small compared to unity. This cannot be the case uniformly for our twisted ansatz, where the fields near $x = L$ take values close to $\mathrm{e}^{\pm\mathrm{i}\theta}/\sqrt{3}$. Still, the fact that $\mathsf{I}(x+1/2)$ depends *linearly* on the position is encouraging: this is exactly the behavior we expect for the *phases* of the fields in the ansatz.

The linearization of the saddle-point equations can actually be performed near *any* of the degenerate family of vacua (45). Linearizing the equations in the vicinity of a vacuum $v = \mathrm{e}^{\pm\mathrm{i}\varphi}/\sqrt{3}$, we obtain for the deviations the same transfer matrix as before. We can therefore construct local solutions near various φ-vacua using (54), and glue them together to obtain a global, "rotating" solution. An equivalent procedure is to exponentiate the deviations,

$$v_0(x) = \frac{1}{\sqrt{3}} \exp\{\delta v_0(x)\}, \tag{55}$$

etc., and extend Eq. (54) for $\mathsf{I}(x+1/2)$ to a larger domain of validity. This we do as follows.

First of all, the R-part of the deviations grows exponentially, and is staggered with respect to x. Our ansatz excludes both features, so we simply set $c_{+r} = c_{-r} = 0$. Next, we note that the I-deviations depend on two coefficients, c_{+i} and c_{-i}. According to (55), their real parts describe the moduli of the fields, and the imaginary parts the phases. In our ansatz, we expect the moduli of the fields to be constant and close to $1/\sqrt{3}$ (a linear growth would be incompatible with the boundary conditions). Therefore, we set $\operatorname{Re} c_{+i} = 0$.

The other coefficient c_{-i} causes a global shift of the fields, which can be interpreted as a "generalized chiral rotation": the generalization consists in taking in Eqs. (30) for U_1

and U_2 any *invertible complex matrix*, and replacing $U_1^\dagger$ and $U_2^\dagger$ by U_1^{-1} and U_2^{-1}. One easily checks that the effective action is invariant under this $\mathrm{GL}(N_f) \times \mathrm{GL}(N_f)$ extension of the chiral symmetry group. The complex extension appears since we have relaxed the Hermiticity condition. The parameter c_{-i} is then seen to parametrize the $\mathbb{C}^\times$-manifold of scalar complex homogeneous vacua.

The remaining coefficient, which we abbreviate to $\alpha \overset{\text{def}}{=} \mathrm{Im}\, c_{+i}$, is responsible for a non-homogeneous solution. As we explained above, deviations $l(x) \sim i\alpha x$ of order $\mathcal{O}(1)$ can be rescaled to deviations of order $\mathcal{O}(\alpha)$ by changing the reference vacuum $e^{\pm i\varphi}/\sqrt{3}$. As a result, the fields built from (55), (54) with $c_{\pm r} = 0$, $\mathrm{Re}\, c_{+i} = 0$ satisfy the saddle-point equations up to order $\mathcal{O}(\alpha^2)$ uniformly in x.

One can add terms of higher order in α to the exponent, so as to kill the higher-order terms in the expansion of (47). By iterating the procedure, one obtains for the fields a series expansion in powers of α, such that the saddle-point equations are satisfied to any order. We conjecture that this expansion can be (re)summed, at least in a certain domain in α, thereby yielding an exact solution of (47). The solution up to order α^2 is

$$v_0(x) = \frac{e^{i\alpha x}}{\sqrt{3}} e^{c_{-i} - i\alpha/2 + 5\alpha^2/8},$$

$$v_1(x + 1/2) = \frac{e^{i\alpha x}}{\sqrt{3}} e^{c_{-i} + i\alpha - \alpha^2/8},$$

$$v_1^*(x + 1/2) = \frac{e^{-i\alpha x}}{\sqrt{3}} e^{-c_{-i} + i\alpha - \alpha^2/8}. \tag{56}$$

The expressions for the fields w, w^* are obtained by replacing $\alpha \to -\alpha$, $c_{-i} \to -c_{-i}$.

The coefficient α parametrizes the slope of the phase with respect to x, and it must be tuned according to the boundary conditions:

$$\alpha L = \theta + 2\pi Q_w, \tag{57}$$

where Q_w is some integer. For a finite twist θ, α can be chosen small only in the large–volume limit $L \gg 1$, in which case α can take several values labeled by the integers $Q_w \ll L$.

4.2.4. Topologically non-trivial configurations

We now return to the original problem with periodic boundary conditions ($\theta = 0$). We have shown that there exist non-trivial solutions, for which the fields are position-dependent, with their phases rotating Q_w times when the position x goes from 0 to L. The integer Q_w can be called the *winding number* of the configuration. We can associate a winding number to a (discrete) configuration because the phases of the fields v, w are varying *smoothly* with position. More generally, when the lattice has the topology of a $(1 + d)$-dimensional torus, one can associate to any smooth scalar configuration a set of winding numbers $\{Q_{w,\hat{\mu}}\}$, each number specifying the number of times $\arg(v)$ rotates between the positions $(n + \frac{\hat{\nu}}{2})$ and $(n + L\hat{\mu} + \frac{\hat{\nu}}{2})$.

Using Newton's algorithm, we have searched for numerical solutions of the vacuum saddle-point equations (47), starting from trial configurations with $Q_w = 1$, $Q_w = 2$. We
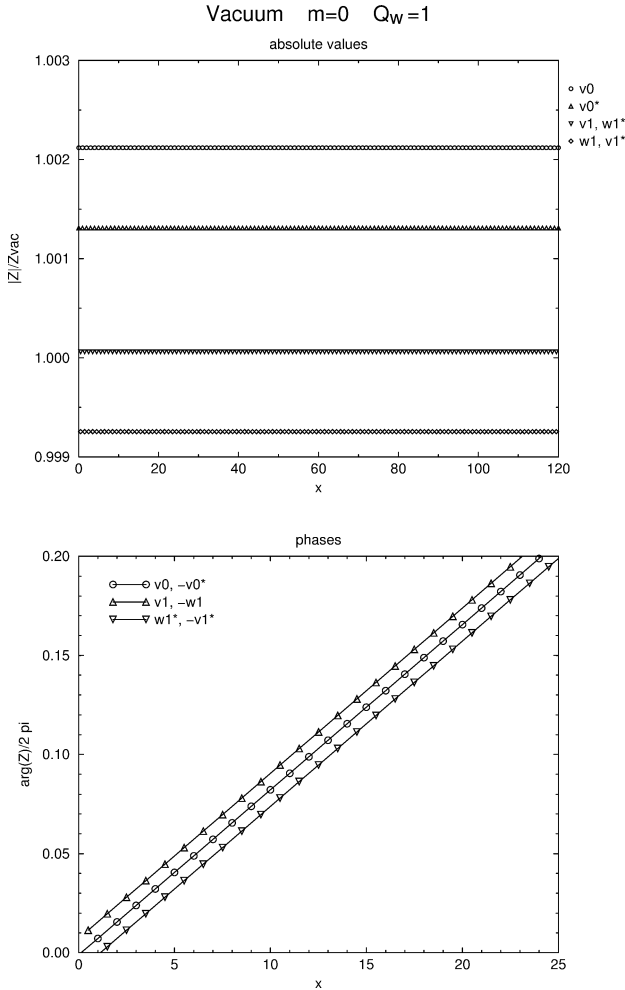
Fig. 3. Vacuum configuration computed numerically, with winding number $Q_w = 1$ in the chiral limit. Fields which are numerically indistinguishable (e.g., $|v_1|$ and $|w_1^*|$) are represented by the same symbol. There is a perfect fit with formulas (56), including the α^2 correction. The difference between $|v_0|$ and $|v_0^*|$ comes from $\mathrm{Re}\, c_{-i} \neq 0$.

plot some results in Fig. 3. These plots are very well described by our approximation (56), including the $\mathcal{O}(\alpha^2)$ corrections.

4.2.5. Nontrivial vacua for finite quark mass

So far we have constructed non-trivial vacua only in the chiral limit, where a continuum of homogeneous vacuum configurations exists. What happens to these non-trivial vacua when the chiral symmetry is broken explicitly by switching on the quark mass?

Recall that for $m \neq 0$ there remain only two homogeneous scalar vacua (43) out of the former U(1) continuum, with one of them ($z_{\mathrm{vac}} = z_+$) being an absolute minimum of

the action. One can again study the linearized saddle-point equations near this solution. Unlike before, the results will apply only locally, since we cannot use the trick of rescaling the homogeneous reference vacuum any more.

We have performed numerical searches for $(1 + 1)$-dimensional topologically non-trivial vacua, assuming the same symmetries as before (we took scalar, time-independent, smoothly varying fields). The saddle-point equations are modified by the addition of the quark mass term $2am$ to the left-hand side of Eq. (47). The outcome of these calculations (see below) can be understood in large part by analytical reasoning, as follows.

To linearize the saddle-point equations around the point z_+, we set

$$v_0(x) = z_+ e^{\delta v_0(x)}, \quad \text{etc.} \tag{58}$$

As in the chiral case, the 4×4 transfer matrix splits into two 2×2 matrices that apply to the vectors R, I defined in Eq. (48). These matrices can be written for an arbitrary value of am, using the exact expression (43) for $z_+(am)$ (we only consider the case $d = 1$). Using the same notations as above, they are

$$\mathsf{T}_r(am) = \frac{1}{1 - z_+^4} \begin{pmatrix} -z_+^{-2} - 2 - z_+^2 & 2z_+^2 + 2z_+^4 \\ -2z_+^2 - 2z_+^4 & -z_+^2 + 2z_+^4 + 3z_+^6 \end{pmatrix},$$

$$\mathsf{T}_i(am) = \frac{1}{1 - z_+^4} \begin{pmatrix} z_+^{-2} - 2 + z_+^2 & 2z_+^2 - 2z_+^4 \\ -2z_+^2 + 2z_+^4 & z_+^2 + 2z_+^4 - 3z_+^6 \end{pmatrix}, \tag{59}$$

and the deviations on links pointing in the time direction propagate as

$$\begin{pmatrix} \delta v_0(x) \\ \delta v_0^*(x) \end{pmatrix} = \frac{1}{2(1 - z_+^2)} \begin{pmatrix} 1 & -z_+^2 \\ 1 & -z_+^2 \end{pmatrix} \mathsf{R}(x - 1/2)$$

$$+ \frac{1}{2(1 + z_+^2)} \begin{pmatrix} 1 & -z_+^2 \\ -1 & z_+^2 \end{pmatrix} \mathsf{I}(x - 1/2). \tag{60}$$

One easily checks that both transfer matrices have the property $\text{Det}\,\mathsf{T}_{r/i}(am) = 1$.

We expand both matrices and their spectra in powers of am, since we are interested in the case of a small quark mass. In the massless limit the matrix $\mathsf{T}_r(0)$ is hyperbolic, with negative real eigenvalues that are well separated from each other (one expanding, the other contracting). Thus, a perturbation of order $\mathcal{O}(am)$ is still diagonalizable, with eigenvalues and eigenspaces shifted by that same order $\mathcal{O}(am)$. We will keep calling the eigenvalues $-e^{\pm\lambda}$, with the expansion

$$\lambda(am) = \ln(3 + 2\sqrt{2}) + am/\sqrt{6} + \mathcal{O}\big((am)^2\big). \tag{61}$$

On the other hand, $\mathsf{T}_i(0)$ was non-diagonalizable with eigenvalue $+1$, so a perturbation can change its qualitative features. For any positive am, $\mathsf{T}_i(am)$ becomes diagonalizable, with real positive eigenvalues $e^{\pm\gamma(am)}$ associated to eigenvectors $\binom{1}{e^{\pm\kappa_1(am)}}$. To express the deviations of the field $v_0(x)$, we use the coefficients

$$e^{\kappa\pm 0} \overset{\text{def}}{=} \frac{1 + z_+^2 e^{\pm\kappa_1}}{1 + z_+^2}.$$

For small am, these data have the following expansions:

$$\gamma(am) = \frac{2}{3^{1/4}}(am)^{1/2} + \frac{5}{3^{7/4}}(am)^{3/2} + \mathcal{O}\big((am)^{5/2}\big),$$

$$\kappa_1(am) = -\frac{4}{3^{1/4}}(am)^{1/2} - \frac{4}{3^{7/4}}(am)^{3/2} + \mathcal{O}\big((am)^{5/2}\big),$$

$$\kappa_{\pm 0}(am) = \mp\frac{1}{3^{1/4}}(am)^{1/2} + \frac{\sqrt{3}}{2}am \pm \frac{1}{2 \times 3^{7/4}}(am)^{3/2} + \mathcal{O}\big((am)^{2}\big). \qquad (62)$$

For a finite mass am, one expects the linear approximation to be valid only for small deviations. However, the error introduced in the saddle-point equations by the linear approximation is at most of order $\mathcal{O}(am|\delta z|)$, so it remains small if the mass is small.

The numerical solution we obtained for a mass $am = 0.01$ and winding number $Q_w = 1$ (see Figs. 4, 5) suggest that the vectors R are negligible in a large domain of x around the point $x = 0$ where fields are close to z_+. This indicates that the coefficients $c_{\pm r}$ vanish, like in the chiral case. The fields will, therefore, depend on two complex parameters $\epsilon_\pm$:

$$\delta v_1(x + 1/2) = \epsilon_+ e^{\gamma x} + \epsilon_- e^{-\gamma x},$$

$$\delta v_1^*(x + 1/2) = -\epsilon_+ e^{\kappa_1 + \gamma x} - \epsilon_- e^{-\kappa_1 - \gamma x},$$

$$\delta v_0(x + 1) = \epsilon_+ e^{\kappa_{+0} + \gamma x} + \epsilon_- e^{\kappa_{-0} - \gamma x}. \qquad (63)$$

As opposed to the chiral case, both coefficients $\epsilon_\pm$ are complex, so that both the phases and the moduli of the fields vary with x. This ansatz fits the numerical solution even when the deviations from z_+ become of order $\mathcal{O}(1)$, which is quite surprising. However, it is unable to reproduce the zone where the fields cross the negative real axis (near $x = L/2$). For a quark mass $am = 0.01$ the values of the various exponents are

$$\gamma = 0.1527, \qquad \kappa_1 = -0.3045, \quad \kappa_{+0} = -0.0673, \qquad \kappa_{-0} = 0.0845. \qquad (64)$$

These values are used in the fits to the numerical solution shown in Fig. 5.

5. Static baryon saddle-point equations

The effective action S_{baryon} for the static-baryon sector, Eq. (37), contains a "string" term in addition to the "sea" term $S_{|0\rangle}$. While the sea term depends on every one of the matrices $Z(n + \frac{\hat{\mu}}{2})$, the string term involves only those matrices Z and $Z^\dagger$ that are situated in the near vicinity of the string. More precisely, what enters into the baryon world line propagator, G, are the matrices $N((t + \frac{1}{2})\hat{0})$ and $M(t\hat{0})$. Of these, the former depend only on Z and $Z^\dagger$ along the string, whereas the latter also involve the matrices $Z(t\hat{0} + \hat{\mu}/2)$ and $Z^\dagger(t\hat{0} - \hat{\mu}/2)$. The Z field on the remaining links (away from the string) appears only in $S_{|0\rangle}$, so the variation with respect to these matrices yields the same Eqs. (40) and (41) as in the vacuum sector.

For simplicity let us consider the two particular cases $N_c = 2$ and $N_c = 3$, using the expressions (39) for the effective action. The most general variation yields

$$N_c = 2 : \delta S_{\text{baryon}} = \delta S_{\text{vacuum}} - \frac{\text{Tr}(\mathsf{G}\delta\mathsf{G}) + \text{Tr}(\mathsf{G})\,\text{Tr}(\delta\mathsf{G})}{\text{Tr}(\mathsf{G}^2) + (\text{Tr}\,\mathsf{G})^2},$$
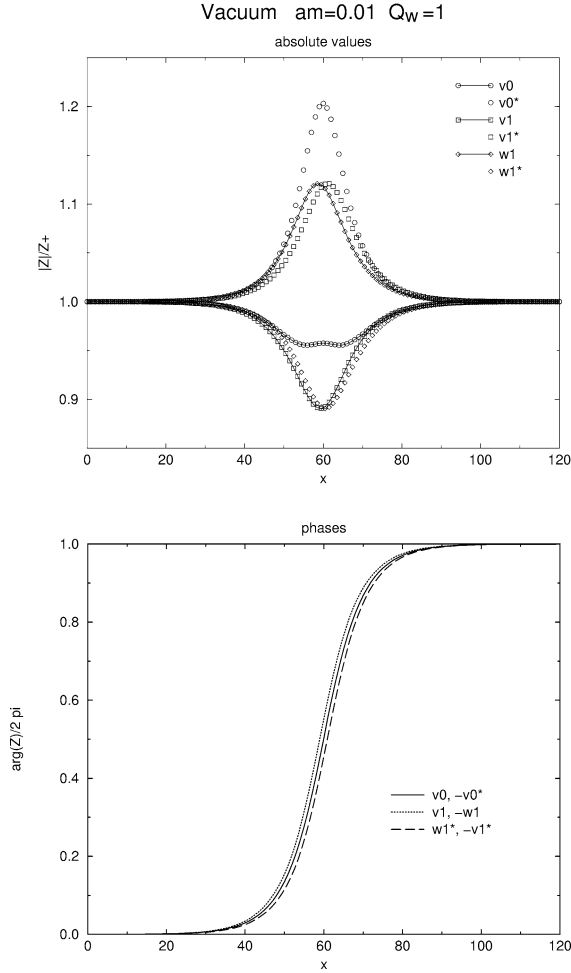
Vacuum   am=0.01 $Q_W = 1$

Fig. 4. Numerical vacuum configuration with winding number $Q_w = 1$ and chiral symmetry explicitly broken by a finite quark mass. The fields are normalized with respect to the corresponding value z_+. The phases $\arg(v_0)$ and $-\arg(v_0^*)$ are indistinguishable, so we plot them together (idem for $\arg(v_1)$ and $-\arg(w_1)$, respectively, $\arg(w_1^*)$ and $-\arg(v_1^*)$).

$$N_c = 3 : \delta S_{\text{baryon}}$$

$$= \delta S_{\text{vacuum}} - \frac{(\text{Tr}\,\mathsf{G})^2\,\text{Tr}\,\delta\mathsf{G} + 2\,\text{Tr}\,\mathsf{G}\,\text{Tr}(\mathsf{G}\delta\mathsf{G}) + \text{Tr}(\mathsf{G}^2)\,\text{Tr}(\delta\mathsf{G}) + 2\,\text{Tr}(\mathsf{G}^2\delta\mathsf{G})}{(\text{Tr}\,\mathsf{G})^3 + 3\,\text{Tr}\,\mathsf{G}\,\text{Tr}(\mathsf{G}^2) + 2\,\text{Tr}\,\mathsf{G}^3}.$$

We then work out how the various traces of powers of G respond to variations of each matrix Z and $Z^\dagger$ entering in the definition of G. For instance, variations of $Z(t\hat{0} + \hat{\mu}/2)$ with $\mu \neq 0$ affect only the matrix $M(t\hat{0})$, whereas varying $Z((t + 1/2)\hat{0})$ affects both $M(t\hat{0})$ and $N((t + 1/2)\hat{0})$. These computations are simplified by the use of cyclicity
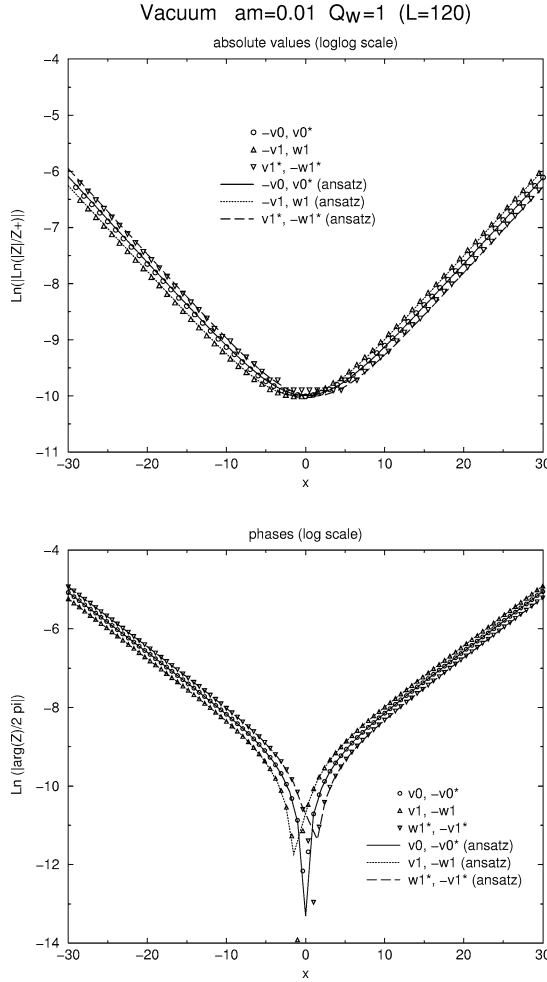
Vacuum　am=0.01　Q_W=1　(L=120)

Fig. 5. Same vacuum configuration as in the previous figure, plotted on a logarithmic scale. We fit the fields in the range $0 < |x| < 30$ (where they are close to z_+) with the ansatz (63), using the theoretical values for γ, κ_1, $\kappa_{\pm 0}$ from Eq. (64). The best fit is obtained with $\epsilon_+ = (-2.80 + \text{i}7.62) \times 10^{-5}$ and $\epsilon_- = (-1.82 - \text{i}5.48) \times 10^{-5}$.

properties: given any decomposition $\mathsf{G} = \mathsf{G}_1 \mathsf{G}_2$, we may replace G in the static-baryon action by the matrix $\widetilde{\mathsf{G}} = \mathsf{G}_2 \mathsf{G}_1$, as G always appears under a trace.

We provide detailed calculations for the variation with respect to $\zeta \equiv Z((t + 1/2)\hat{0})$. The modified factors of G in this case are $M(t\hat{0})^{-1}$ and $N((t + 1/2)\hat{0})$, and the modified matrix G reads

$$\mathsf{G} + \delta\mathsf{G} = \cdots M(t\hat{0})^{-1} \left\{ 1 + \delta\zeta \left[-M(t\hat{0})^{-1} + \zeta^\dagger N\big((t + 1/2)\hat{0}\big)^{-1} \right] \right\}$$
$$\times N\big((t + 1/2)\hat{0}\big) \cdots .$$

It is now natural to conjugate $\mathsf{G} + \delta\mathsf{G}$ into

$$T(\mathsf{G} + \delta\mathsf{G})T^{-1} = \widetilde{\mathsf{G}} + \delta\zeta\left[-M(t\hat{0})^{-1} + \zeta^\dagger N\left((t + 1/2)\hat{0}\right)^{-1}\right]\widetilde{\mathsf{G}},$$

where $\widetilde{\mathsf{G}} \overset{\text{def}}{=} N((t + 1/2)\hat{0})M((t + 1)\hat{0})^{-1} \cdots N((t - 1/2)\hat{0})M(t\hat{0})^{-1}$. The saddle-point equation that follows from varying $Z((t + 1/2)\hat{0})$ then takes the succinct form

$$\delta Z\big((t + 1/2)\hat{0}\big): \quad 0 = \left[-M(t\hat{0})^{-1} + Z^\dagger\big((t + 1/2)\hat{0}\big)N\big((t + 1/2)\hat{0}\big)^{-1}\right]$$
$$\times \big(\mathbb{I}_{N_f} - F_{N_c}(\widetilde{\mathsf{G}})\big),$$

with the case-by-case definition of the matrix-valued function $F_{N_c}(G)$ being

$$N_c = 2 : F_2(G) = \frac{G^2 + G\operatorname{Tr}G}{\operatorname{Tr}(G^2) + (\operatorname{Tr}G)^2},$$
$$N_c = 3 : F_3(G) = \frac{G(\operatorname{Tr}G)^2 + 2G^2\operatorname{Tr}G + G\operatorname{Tr}(G^2) + 2G^3}{(\operatorname{Tr}G)^3 + 3\operatorname{Tr}G\operatorname{Tr}(G^2) + 2\operatorname{Tr}(G^3)}.$$

The saddle-point equation obtained by varying $Z^\dagger((t - 1/2)\hat{0})$ is similar. In terms of the matrix $\widetilde{\mathsf{G}}' = M(t\hat{0})^{-1}N((t + 1/2)\hat{0}) \cdots M((t - 1)\hat{0})^{-1}N((t - 1/2)\hat{0})$ it is best expressed:

$$0 = \big(\mathbb{I}_{N_f} - F_{N_c}(\widetilde{\mathsf{G}}')\big) \cdot \left[-M(t\hat{0})^{-1} + N\big((t - 1/2)\hat{0}\big)^{-1}Z\big((t - 1/2)\hat{0}\big)\right],$$

with the same definitions for F_{N_c} as above. The term multiplying the unit matrix $\mathbb{I}_{N_f}$ stems from δS_{vacuum}. Note that this term factors out in both of the above variations.

To get an idea of the matrix $\mathbb{I}_{N_f} - F_{N_c}(G)$, we compute it in the vacuum configuration $Z \equiv z_{\text{vac}}\mathbb{I}_{N_f}$. In this case we have $\mathsf{G} = \widetilde{\mathsf{G}} = \widetilde{\mathsf{G}}' \propto \mathbb{I}_{N_f}$. We then notice that $F_{N_c}(\alpha\mathbb{I}_{N_f}) = N_f^{-1}\mathbb{I}_{N_f}$ for any number of colors and any $\alpha \neq 0$. Therefore, on the vacuum configuration, we get $\mathbb{I}_{N_f} - F_{N_c}(\mathsf{G}) = (1 - N_f^{-1})\mathbb{I}_{N_f}$, which is invertible as soon as $N_f > 1$. More generally, this equation holds as long as G is a multiple of the unit matrix, which is a property of the inhomogeneous scalar ansatz we will make in the next section.

Clearly, as long as the matrix $\mathbb{I}_{N_f} - F_{N_c}(\mathsf{G})$ remains non-singular, the saddle-point equations due to varying $Z((t + 1/2)\hat{0})$ and $Z^\dagger((t + 1/2)\hat{0})$ are identical to those in the vacuum sector, Eqs. (40) and (41). As was said earlier, this is also the case for the equations due to varying all matrices Z and $Z^\dagger$ not involved in the matrix G, i.e., those away from the string. The only difference to the vacuum equations comes from the matrices on the links *adjacent* to the string, namely $Z(t\hat{0} + \hat{\mu}/2)$, $Z(t\hat{0} - \hat{\mu}/2)$ for the directions $\mu = 1, \ldots, d$. These matrices are contained only in some M^{-1} factor of G, and their variations give the following saddle-point equations:

$$\delta Z(t\hat{0} + \hat{\mu}/2): \quad -M(t\hat{0})^{-1} + Z^\dagger(t\hat{0} + \hat{\mu}/2)N(t\hat{0} + \hat{\mu}/2)^{-1}$$
$$= -M(t\hat{0})^{-1}F_{N_c}(\widetilde{\mathsf{G}}), \tag{65}$$
$$\delta Z^\dagger(t\hat{0} - \hat{\mu}/2): \quad -M(t\hat{0})^{-1} + N^{-1}(t\hat{0} - \hat{\mu}/2)Z(t\hat{0} - \hat{\mu}/2)$$
$$= -F_{N_c}(\widetilde{\mathsf{G}}')M(t\hat{0})^{-1}, \tag{66}$$

where the matrices $\widetilde{\mathsf{G}}$, $\widetilde{\mathsf{G}}'$ are the same as before. These equations represent the only obstruction that prevents the vacuum configuration $Z = Z^\dagger \equiv z_{\mathrm{vac}}\mathbb{I}$ from being also a saddle point of the static-baryon sector.

5.1. Configurations for the static baryon in $1+1$ dimensions

In this section we present approximate solutions of the saddle-point equations in the static baryon sector for the simplest non-trivial case, which is the two-dimensional Euclidean square lattice ($d = 1$). We use the same notations and assume the same symmetries as in Section 4.2.2, so at each position x there are 8 independent complex scalar variables.

The baryonic string is placed on the Euclidean time axis at position $x = 0$. The equations to solve are the vacuum saddle-point equations (47) off the string ($x \neq 0$), and the modified equations

$$
\begin{aligned}
v_0(0) &+ w_0^*(0) + v_1(1/2) + w_1^*(-1/2) + 2am \\
&= v_0(0) + 1/v_0^*(0) \\
&= w_0^*(0) + 1/w_0(0) \\
&= \left(1 - N_f^{-1}\right)\left\{v_1(1/2) + 1/v_1^*(1/2)\right\} \\
&= \left(1 - N_f^{-1}\right)\left\{w_1^*(-1/2) + 1/w_1(-1/2)\right\}
\end{aligned}
\tag{67}
$$

on the string, together with the equations obtained by exchanging $v \leftrightarrow w$, $v^* \leftrightarrow w^*$. As in the vacuum sector, these equations imply the identifications $v_0(x) = w_0^*(x)$ and $w_0(x) = v_0^*(x)$ for all x.

5.1.1. Physical requirements

Recall from Section 4.1 that demanding $Z^\dagger$ to be the Hermitian conjugate of Z (and assuming the vacuum saddle-point equations) leads to a homogeneous configuration, where the fields are constant on each sublattice. Such a homogeneous configuration *cannot* satisfy the last two of Eq. (67). To get a solution, we must relax the Hermiticity condition (cf. Section 4.2.1), and consider the fields Z and $Z^\dagger$ as independent variables.

We want the baryon to be a *localized* object, in the sense that a baryonic saddle-point configuration should differ from a vacuum configuration only in some neighborhood of the baryon world line. The baryon can then be interpreted as a spatially localized excitation of this vacuum. A priori, baryon excitations may exist on top of each of the vacua described in Section 4.

In Eq. (67), the number of flavors N_f enters just as a parameter, so one can extend the equations to any real value of N_f. In the limit $N_f = \infty$, we recover the vacuum saddle-point equations. We can therefore obtain a solution of the baryon saddle-point equations by starting from a given vacuum configuration (at $N_f = \infty$), and deforming the configuration by continuous variation of N_f down to its physical value (say $N_f = 2$). Any baryon configuration obtained in this way carries the same topological charge as the vacuum it is associated to.

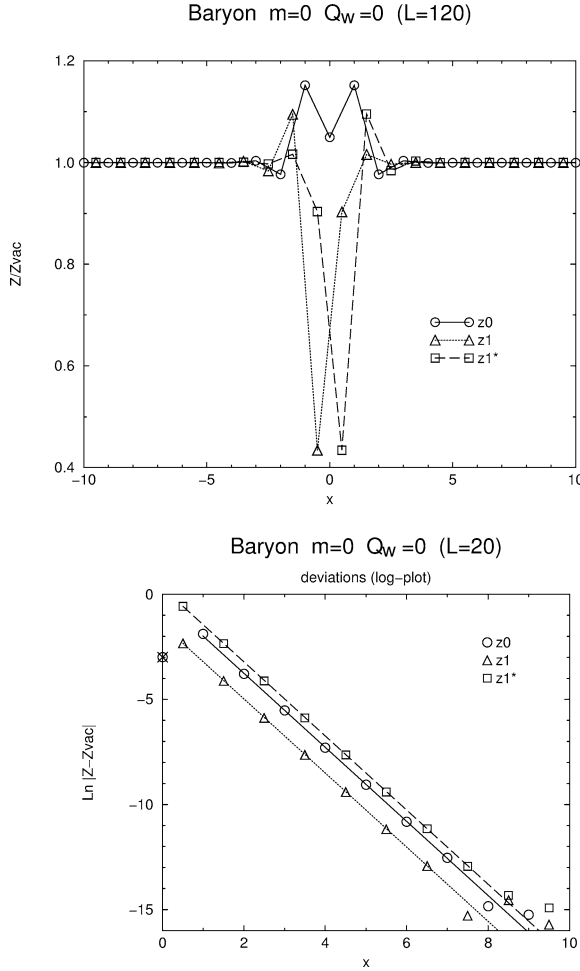Baryon m=0 Q_W =0 (L=120)

Baryon m=0 Q_W =0 (L=20)

Fig. 6. Numerical baryon configuration in the chiral limit. All fields are real. Top: the fields converge exponentially fast to z_{vac}. Bottom: we compare the numerical data (circles, triangles, squares) with the theory of Section 5.1.2 (3 lines, cross for $z_0(0)$).

5.1.2. Topologically trivial sector $Q_w = 0$, chiral limit

In the sector with zero winding number, we numerically found a unique solution (see Fig. 6) asymptotic to the homogeneous vacuum z_{vac}, i.e., satisfying the asymptotic condition

$$v_\mu, \ v_\mu^*, \ w_\mu, \ w_\mu^* \xrightarrow{|x| \to \infty} z_{vac} = 1/\sqrt{3}.$$

All the fields of this configuration are real and time-independent. Various components coincide pairwise or in quadruples:

$$v_0 = w_0 = v_0^* = w_0^* \equiv z_0, \qquad v_1 = w_1 \equiv z_1, \qquad v_1^* = w_1^* \equiv z_1^*.$$

One easily checks that the saddle-point equations are invariant under the following transformation:

$$z_1(x + 1/2) \leftrightarrow z_1^*(-x - 1/2), \qquad z_0(x) \leftrightarrow z_0(-x), \tag{68}$$

which represents a reflection at the baryon world line. The solution found numerically is invariant under this transformation, and we believe the same to be true for the exact solution (or else we would get a second solution by reflection). We can therefore restrict our study to the domain $0 \leqslant x$.

Our numerics show an exponential convergence of all the fields towards z_{vac} as we depart from the string (see Fig. 6), and the signs of the deviations alternate with x. This phenomenon can be explained by the linearized saddle-point equations studied in Section 4.2.3. The linear theory indeed applies if the fields are close to z_{vac}, which is the case for large enough x. Eqs. (51), (54), together with the physical condition that the deviations decay as $x \to \infty$, require $c_{+r} = 0$. We thus get the ansatz

$$z_0(x) = \frac{1}{\sqrt{3}}\Big[1 + c_{-r}\,\sqrt{2}\,e^\lambda\left(-e^{-\lambda}\right)^x\Big],$$

$$z_1(x + 1/2) = \frac{1}{\sqrt{3}}\Big[1 + c_{-r}\left(-e^{-\lambda}\right)^x\Big],$$

$$z_1^*(x + 1/2) = \frac{1}{\sqrt{3}}\Big[1 + c_{-r}\,e^\lambda\left(-e^{-\lambda}\right)^x\Big], \tag{69}$$

with $e^\lambda = 3 + 2\sqrt{2}$ as before. According to this linear approximation, the fields oscillate around the asymptotic value z_{vac}, and the amplitude of the oscillations is controlled by a unique coefficient, which we denote by $C_1 \overset{\text{def}}{=} c_{-r}$.

The results (69) fit the numerical configuration not only far from the string (where this is expected), but even down to the baryon string, where the fields deviate significantly from z_{vac}. More precisely, the ansatz fits z_1, z_1^* for all x, whereas z_0 departs from it only at $x = 0$. The value $z_0(0) \overset{\text{def}}{=} \frac{1}{\sqrt{3}}(1 + \widetilde{C}_0)$ together with the parameter C_1 can be computed using the (nonlinear) saddle-point equations on the string (67) and the reflection symmetry (68). We obtain two equations:

$$\widetilde{C}_0^2 + 2C_1\widetilde{C}_0 + 2C_1 + 4\widetilde{C}_0 = 0,$$

$$3e^\lambda C_1^2 + 4e^\lambda \widetilde{C}_0 C_1 + 4\widetilde{C}_0 + C_1\big(3 + 7e^\lambda\big) + 4 = 0.$$

The equations have four pairs of solutions, two real ones and two complex ones, conjugate to one another. The physical solution (which deforms to $C_1 = \widetilde{C}_0 = 0$ as we vary N_f from 2 to ∞) is $C_1 = -0.0971$ and $\widetilde{C}_0 = 0.0504$, giving

$$\sqrt{2}\,e^\lambda C_1 = -0.8002. \tag{70}$$

The relative smallness of these constants (except for the last one, which governs the amplitude $\delta z_0(0)$) may explain why the ansatz works well down to the string.

The above saddle-point configuration is indeed situated outside of the original contour of integration: it is a "complex saddle point" (although all fields have real values).

A contour deformation has to be performed for the variables $i(z_1 - z_1^*)(x)$, which move away from the real axis as $|x|$ decreases.

This ansatz is tailored to the limit $L \to \infty$, but owing to the fast decrease towards z_{vac}, it is already quite good for short lattices. In Fig. 6 (bottom), we show a logarithmic plot of the deviations of the fields from the homogeneous vacuum, for a lattice of total length $L = 20$, as well as the values predicted by the above ansatz.

This configuration might be called a non-topological soliton, cf. [21]. Its characteristic length (in units of the lattice spacing a) is $\lambda^{-1} = 0.5673$, and its mass will be computed in the next section.

This real scalar configuration is just one point on a $U(N_f)$-manifold of solutions, obtained by the action (30) of the chiral symmetry group. For a generic point on this manifold, the configuration is staggered in time. These solutions are saddle-point configurations for $N_f = 2$, and do not depend on the number of colors N_c (which does not appear in the saddle-point equations). However, the value of the action for these configurations does depend on N_c; see the next section.

5.1.3. Topological baryon, chiral limit

We also obtained topologically non-trivial configurations, characterized by a non-vanishing winding number Q_w. In Fig. 7 we plot a solution in the baryon sector with $Q_w = 1$. All fields are scalar, and have the symmetries described in Section 4.2.2.

Away from the string ($x \gg 1$), the moduli of the fields are close to z_{vac}, and the phase varies linearly. In this region, we can apply the linear theory described in Section 4.2.3, in particular the ansatz (55). Now only the coefficient c_{+r} has to vanish, to prevent the deviations from exploding as $x \to \infty$. As in the vacuum case, the coefficient c_{-i} can take any value, yielding only a chiral shift of the fields. We find that $c_{+i} = i\alpha$ is purely imaginary, as in the vacuum. The fields are well fitted by

$$v_1(x + 1/2) = \frac{1}{\sqrt{3}} e^{i\alpha(x+1)} \left[1 + c_{-r} \left(-e^{-\lambda} \right)^x \right], \quad \text{etc.} \tag{71}$$

for positive x. Near the string, the moduli of the fields behave in a similar way as in the non-topological sector, whereas their phases make a small jump β at $x = 0$. Both this jump and the value of c_{-r} can be computed from the full saddle-point equations near the string (see below). The value of the parameter α depends on the height of this jump: α will not be exactly equal to its value in the vacuum, which is $2\pi/L$ for this topological sector, but rather to $(2\pi - \beta)/L$. As a consequence, the convergence of the fields towards the vacuum configuration away from the string will not be exponential, but only linear (the fields coincide at the "antipode" of the baryon, $x = L/2$).

From Fig. 7, we can assume that the above ansatz is still a good approximation for $v_1(1/2)$, and for $v_1^*(1/2)$ up to a phase jump of $\beta/2$. Given this assumption and setting $N_f = 2$, the saddle-point equation on the baryon worldline, $v_0(0) + 1/v_0^*(0) = 1/2\{v_1(1/2) + 1/v_1^*(1/2)\}$, yields two real equations, one of which reads

$$\frac{\sin(3\alpha/2 + \beta/2)}{\sin(\alpha/2)} = \frac{3(1 + C_1)}{2(1 + C_1 e^\lambda)}.$$
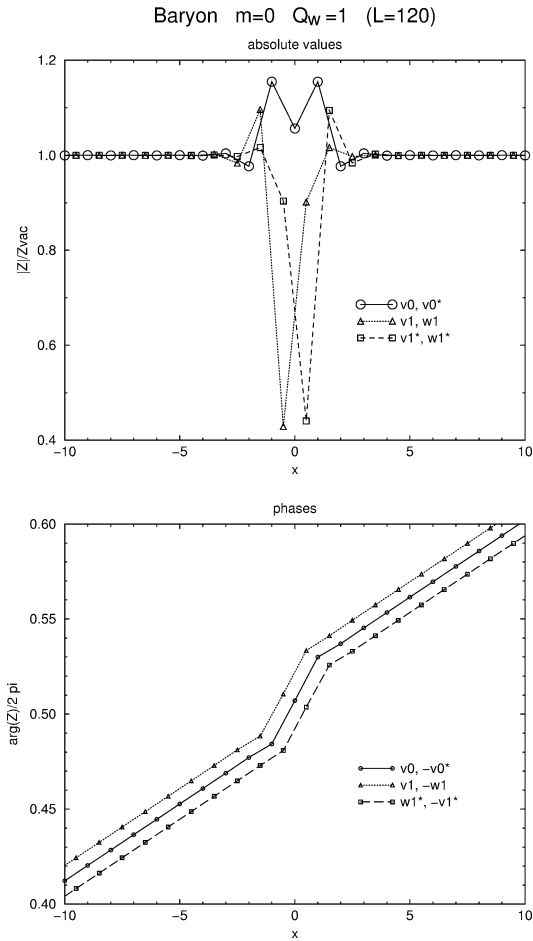
Baryon   m=0 Q_W =1   (L=120)

Fig. 7. Numerical baryon in the chiral limit with winding number $Q_w = 1$ (we only plot the vicinity of the baryon worldline). The absolute values are very similar to the case $Q_w = 0$, but now the phases vary linearly away from the worldline. The slope α and the phase jump β at the baryon are in good agreement with the theory of Section 5.1.3: we find $2\pi/\alpha = 123.42$ and $\arg v_0(1) - \arg v_0(-1) = 0.046 \approx 5.24\alpha$.

For small angles α and β, this equation gives a linear relation between them: using the value for C_1 obtained in the non-topological sector, we get $\beta \approx 3.24\alpha$. The value of the slope α then is $\alpha = 2\pi Q_w/(3.24 + L)$.

5.1.4. Topological baryon, $m \neq 0$

As in the vacuum sector, our results for a finite quark mass are mostly numerical (see Figs. 8, 9). We obtained solutions of the saddle-point equations with various winding numbers, which are close to the corresponding vacuum configurations except in the vicinity of the baryon string. Near the antipode of the string ($x = L/2$), the field approaches the
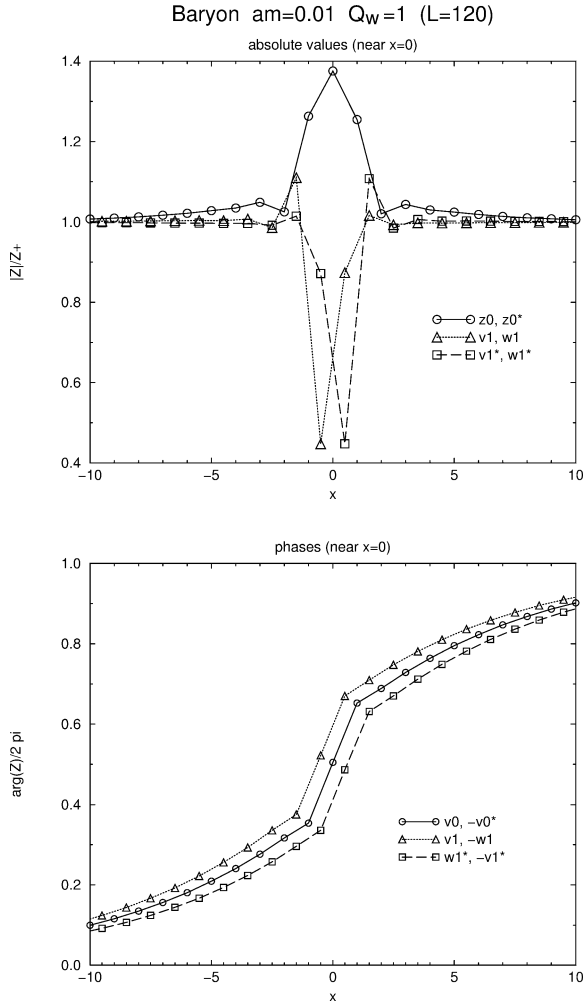
Fig. 8. Numerical baryon with winding number $Q_w = 1$ and broken chiral symmetry. Away from the worldline, the fields converge exponentially fast to z_+. The logarithms of the phases are linear in the range $3 < x < 55$, with slopes $0.1523 \leqslant \gamma \leqslant 0.1533$ in agreement with the theoretical value from Eqs. (64).

homogeneous value z_+, and the fields can be fitted by the linear theory developed in Section 4.2.5.

6. Mass of the static baryon ($N_f = 2$)

The mass M_{baryon} of the baryon is defined by comparing the static baryon partition function to the vacuum one. Since the saddle-point configurations are classified according
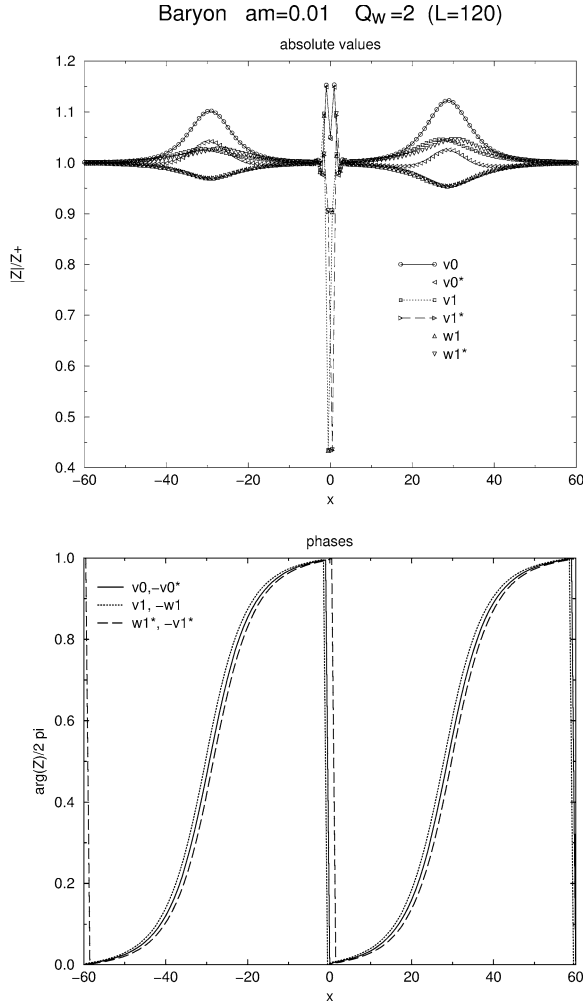
Fig. 9. Numerical baryon with winding number $Q_w = 2$ and broken chiral symmetry. The symmetry with respect to $x = 0$ is only approximate, due to a numerical loss of accuracy.

their winding number Q_w, the comparison is performed within a given topological class, i.e., between a baryon configuration and the corresponding vacuum sector.

In the limit of large lattices, the ratio of partition functions is expected to behave as

$$\frac{\mathcal{Z}_{\text{baryon}, Q_w}(L \times T)}{\mathcal{Z}_{\text{vacuum}, Q_w}(L \times T)} \propto e^{-M_{\text{baryon}, Q_w} T} \quad \text{as } T \to \infty. \tag{72}$$

As explained in Section 3.2, we estimate both partition functions through their respective lowest-order saddle-point approximations:

$$\frac{\mathcal{Z}_{\text{baryon}}}{\mathcal{Z}_{\text{vacuum}}} \sim \exp\left(-N_c\left\{S_{\text{baryon}}[z_{\text{baryon}}] - S_{\text{vacuum}}[z_{\text{vac}}]\right\}\right). \tag{73}$$

As before, we will only treat the $(1 + 1)$-dimensional case.

6.1. Mass of the static non-topological baryon

We first study the baryonic excitation on top of a homogeneous vacuum, which has vanishing winding number. The value of the action for the homogeneous vacuum was given in Eq. (44). It is proportional to the volume of the lattice, and is called a "sea" term in the literature.

The action S_{vacuum} is part of the full static baryon action (37), which leads to a "sea" contribution to the baryon mass:

$$M_{\text{sea}} \overset{\text{def}}{=} N_c \frac{S_{\text{vacuum}}[z_{\text{baryon}}] - S_{\text{vacuum}}[z_{\text{vac}}]}{T}.$$

We now assume the limit $m = 0$ (Section 5.1.2). By the time-independence of both configurations, the sea contribution reads

$$M_{\text{sea}} = N_f N_c \left(\sum_{x=-L/2}^{L/2} \ln \frac{N_1(x + 1/2)N_0(x)}{M(x)} \bigg|_{Z=z_{\text{baryon}}} \right.$$
$$\left. - \ln \frac{N_1(x + 1/2)N_0(x)}{M(x)} \bigg|_{Z=z_{\text{vac}}} \right).$$

Since the deviations of the fields from z_{vac} are small and decrease exponentially—see Eq. (69)—it is reasonable to keep only the linear order, and extend the sums to $L = \infty$. Quite remarkably, this linear approximation gives a *vanishing* sea term (for $m = 0$). Alternatively, we can compute the sea term from the $N_f = 2$ configuration obtained numerically. In this way we obtain

$$M_{\text{sea}} \approx 0.02324 \times N_c \ \left(\text{in units of } a^{-1}\right).$$

This answer is small (5%) compared to the second term we compute below, so the linear approximation (giving $M_{\text{sea}} = 0$) is rather good in this respect.

The remaining contribution to the baryon mass comes from the sum over traces of G, which involve only the fields on or adjacent to the string. In the QCD context this is generally referred to as the "valence quark contribution" [21]. For the time-independent configuration described in Section 5.1.2, the valence term for $N_f = 2$ becomes

$$M_{\text{valence}} = \ln \left\{ \frac{\alpha_0}{\alpha_1} \binom{N_c + N_f - 1}{N_c} \right\} + N_c \ln \left(\frac{2z_0(0) + 2z_1(1/2)}{1 + z_0(0)^2} \right) \bigg|_{z_{\text{bar}}}. \tag{74}$$

The term proportional to N_c evaluates to

$$\ln \sqrt{3} \ + \ \ln \left(\frac{1 + C_1/2 + \widetilde{C}_0/2}{1 + \widetilde{C}_0/2 + \widetilde{C}_0^2/4} \right) \approx \ln \sqrt{3} \ + \ C_1/2 = 0.5493 - 0.0485.$$

We notice that the second term due to the deviations $|z_{\text{baryon}} - z_{\text{vac}}|$ is small compared to the first term $\ln \sqrt{3}$, obtained by inserting the vacuum configuration z_{vac} into (74).

Table 1

Q_w	$m = 0$	$am = 0.002$	$am = 0.01$
0	2.839	2.840	2.852
1	2.840	3.097	3.692

The result of this linear approximation is very close to the exact (numerical) value, 0.5004. On including the combinatorial and normalization terms (see Eq. (B.7)), we finally get, for the non-topological static baryon in the chiral limit:

$$M_{\text{baryon}} \approx 0.5236 N_c + \ln(1 + N_c/2) + \ln(1 + N_c). \tag{75}$$

This yields for example

$$N_c = 2 : M_{\text{baryon}} = 2.839 \, a^{-1},$$
$$N_c = 3 : M_{\text{baryon}} = 3.873 \, a^{-1},$$

where we have reinstated the mass scale given by the lattice constant.

6.2. Masses of topological baryons

To compute the baryon masses in the topologically non-trivial sectors, we first need to evaluate S_{vacuum} on the corresponding vacua with winding number Q_w. This is straightforward in the chiral limit, where we have the accurate approximation (56) at our disposal. The result up to second order in the small parameter $\alpha = 2\pi Q_w/L$ is

$$T^{-1}\big(S_{\text{vacuum}}[z_{\text{vac},\alpha}] - S_{\text{vacuum}}[z_{\text{vac}}]\big) = N_f L \frac{3\alpha^2}{16} = \frac{3\pi^2 Q_w^2}{4L} N_f.$$

The vacuum energies are obtained from this by multiplication with the number of colors, N_c. They agree well with the values computed numerically for $L = 120$ (and $N_c = 2$): $E_1^{(0)} = 0.25$, $E_2^{(0)} = 0.98$.

The baryon mass in each topological sector is defined relative to the corresponding vacuum energy $E_{Q_w}^{(0)}$. For a non-vanishing quark mass, both the vacuum energy and the baryon energy are computed numerically. In Table 1, we summarize our results for a lattice $L = 120$, with $N_c = N_f = 2$, for various quark masses: In Fig. 10, we plot the baryon masses in the topological sectors $Q_w = 0$ and $Q_w = 1$ as a function of the quark mass.

7. Zigzag baryon

In the standard formulation of the theory on the Euclidean 2-dimensional square lattice, the temporal and spatial directions are given by the lattice generators, $\hat{t} = (1, 0)$, $\hat{x} = (0, 1)$. However, it is also possible to use different spacetime axes. For instance, on the same square lattice, we define the *zigzag* spacetime axes as $\hat{t} = (1/2, -1/2)$, $\hat{x} = (1/2, 1/2)$ (see Fig. 11). The unit spacetime separation now has the length $a/\sqrt{2}$. For convenience, we choose the spacetime origin on the *middle of a link* (say, a link in the direction $\hat{t} + \hat{x}$),
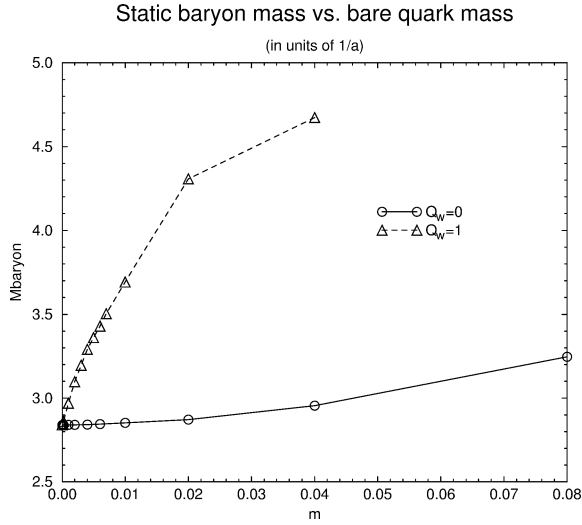
Static baryon mass vs. bare quark mass

Fig. 10. Masses of static baryons as functions of the quark mass am, for the topological sectors $Q_W = 0$ and $Q_W = 1$.
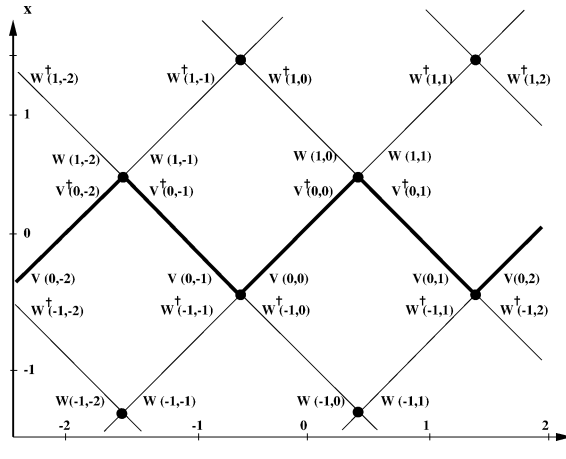

Fig. 11. Zigzag baryon string on a square lattice.

so that the coordinates of lattice sites will be half-integers, while links will be indexed by integers.

The division of the square lattice into two sublattices is now expressed only in terms of the spatial coordinate: the links at *even* positions $x = 2n$ carry the fields $V, V^{\dagger}$, while the links at odd $x = 2n + 1$ carry the fields $W, W^{\dagger}$.

The vacuum effective action and its corresponding saddle-point equations are still given by the formulas (40), (41), after a suitable change of labels for links and sites.

7.1. Time-independent vacua

Once again, we make a scalar time-independent ansatz for the fields:

$$\forall x \text{ even}, \ \forall t: \quad V(x,t) = v(x)\mathbb{I}, \qquad V^\dagger(x,t) = v^*(x)\mathbb{I}, \tag{76}$$

$$\forall x \text{ odd}, \ \forall t: \quad W(x,t) = w(x)\mathbb{I}, \qquad W^\dagger(x,t) = w^*(x)\mathbb{I}. \tag{77}$$

In particular, this implies the equality of fields situated on links (x,t) and $(x,t+1)$. There are 2 scalar variables at each position.

With these symmetries, the vacuum saddle-point equations read:

$$
\begin{aligned}
x \text{ even}: \quad 2v(x) + 2w^*(x-1) + 2am &= v(x) + 1/v^*(x) \\
&= w^*(x-1) + 1/w(x-1), \\
x \text{ odd}: \quad 2w(x) + 2v^*(x-1) + 2am &= w(x) + 1/w^*(x) \\
&= v^*(x-1) + 1/v(x-1).
\end{aligned}
\tag{78}
$$

In the chiral limit, the homogeneous vacuum configurations are still given by $v = w^* = e^{i\varphi} z_{\text{vac}}$ and $v^* = w = e^{-i\varphi} z_{\text{vac}}$. For fields close to this vacuum ($v(x) = e^{i\varphi} z_{\text{vac}} \exp\{\delta v(x)\}$, etc.) the linearized saddle-point equations yield the following transfer matrix equation:

$$
\begin{pmatrix} \delta z(x) \\ \delta z^*(x) \end{pmatrix} = \begin{pmatrix} -3/2 & -1/2 \\ 1/2 & -1/2 \end{pmatrix} \begin{pmatrix} \delta z(x-1) \\ \delta z^*(x-1) \end{pmatrix} = \mathsf{T}_{\text{zig}} \begin{pmatrix} \delta z(x-1) \\ \delta z^*(x-1) \end{pmatrix}. \tag{79}
$$

The symbol δz stands for either δv or δw, depending of the parity of x. In contrast with Section 4.2.3, we now have just one transfer matrix, which relates deviations of v, v^* to deviations of w, w^* and vice versa. This transfer matrix T_{zig} is related to the matrix T_i described in Section 4.2.3. Indeed, it acts on the vectors l_+, l_- as follows:

$$\mathsf{T}_{\text{zig}} \mathsf{l}_+ = -\mathsf{l}_+ - \mathsf{l}_-, \qquad \mathsf{T}_{\text{zig}} \mathsf{l}_- = -\mathsf{l}_-.$$

The deviations $\delta v(0)$, $\delta v^*(0)$ are parametrized by two *complex* parameters $c_\pm$ as

$$\begin{pmatrix} \delta v(0) \\ \delta v^*(0) \end{pmatrix} = c_+ \mathsf{l}_+ + c_- \mathsf{l}_-.$$

The deviations will then depend on position as follows (x is even):

$$
\begin{pmatrix} \delta v(x) \\ \delta v^*(x) \end{pmatrix} = \begin{pmatrix} c_- + (x+1)c_+ \\ -c_- - (x-1)c_+ \end{pmatrix}, \qquad
\begin{pmatrix} \delta w(x+1) \\ \delta w^*(x+1) \end{pmatrix} = \begin{pmatrix} -c_- - (x+2)c_+ \\ c_- + x c_+ \end{pmatrix}.
\tag{80}
$$

The rest of the discussion is identical to the one following Eq. (55). The coefficient c_- plays the role of a global shift, or "generalized chiral rotation". If $\operatorname{Re} c_+ \neq 0$, the absolute values of the fields vary linearly with x, which is incompatible with their periodicity. On the other hand, taking $c_+ = i\alpha$ will linearly rotate the phases of the fields, keeping them close to some vacuum configuration, as in Eq. (56). Taking for α a multiple of $2\pi/L$, we obtain a topologically non-trivial configuration.

The case of broken chiral symmetry ($m \neq 0$) can be treated along the same lines as in Section 4.2.5; the above linear evolution in position is then replaced by an exponential

one, at least for fields in the vicinity of the value z_+. The transfer matrix takes the form $\begin{pmatrix} -z_+^{-2}/2 & -1/2 \\ 1/2 & -3z_+^2/2 \end{pmatrix}$, and has the eigenvalues $-\exp(\pm\gamma_{\text{zig}})$ associated to the eigenvectors $\begin{pmatrix} 1 \\ -\exp(\pm\kappa_{\text{zig}}) \end{pmatrix}$, with the expansions

$$\gamma_{\text{zig}} = \frac{\sqrt{2}}{3^{1/4}}(am)^{1/2} + \mathcal{O}\big((am)^{3/2}\big), \tag{81}$$

$$\kappa_{\text{zig}} = -\frac{2\sqrt{2}}{3^{1/4}}(am)^{1/2} + \mathcal{O}\big((am)^{3/2}\big). \tag{82}$$

Up to this order, the exponent γ_{zig} differs from the corresponding exponent γ of Eq. (62) by a factor of $\sqrt{2}$. This factor actually compensates for the ratio of unit lengths between the two frameworks (a versus $a/\sqrt{2}$). For the quark mass $am = 0.005$ used in compiling the figures, we have $\gamma_{\text{zig}} = 0.0762$ and $e^{\kappa_{\text{zig}}} = 0.85905$.

7.2. Zigzag baryon configurations

In the new labeling conventions, the worldline of a static baryon situated at position $x = 0$ forms a zigzag curve (see Fig. 11). Assuming that the fields are scalar and time-independent, the G matrix appearing in the baryonic part of the action is

$$\mathsf{G} = \big\{\big[2v(0) + 2w^*(-1) + 2am\big]^{-1}\big(1 + v(0)v^*(0)\big)$$
$$\times \big[2w(1) + 2v^*(0) + 2am\big]\big(1 + v(0)v^*(0)\big)\big\}^{T/2}\,\mathbb{I}.$$

The resulting saddle-point equations on the string read

$$2v(0) + 2w^*(-1) + 2am = v(0) + 1/v^*(0)$$
$$= \big(1 - N_f^{-1}\big)\big\{w^*(-1) + 1/w(-1)\big\},$$
$$2w(1) + 2v^*(0) + 2am = v^*(0) + 1/v(0)$$
$$= \big(1 - N_f^{-1}\big)\big\{w(1) + 1/w^*(1)\big\}. \tag{83}$$

The saddle-point equations are invariant under the transformation

$$w(-x) \longleftrightarrow w^*(x), \qquad v(-x) \longleftrightarrow v^*(x), \tag{84}$$

which is also a symmetry of our numerical solutions.

In the chiral limit, the linear dependence in (80) makes it impossible for the absolute values of the fields to approach z_{vac} at infinity, unless the deviations are purely imaginary; this latter possibility ($|z(x)| \equiv z_{\text{vac}}$) is incompatible with the saddle-point equations on the baryon string (83). However, for a finite lattice, infinity is the "antipodal point" $x_\infty = \pm L/2$. In numerical searches (see Fig. 12, top), we found a solution which comes close to z_{vac} near the antipode (but does not converge exponentially to it). To describe these fields, it is convenient to use the position variable centered at the antipode, $x' = x + L/2$ (we assume that $L/2$ is even, so that x and x' have the same parity). The symmetry (84) also holds if one replaces x by x'. For x' even, $-L/2 < x < L/2$, the fields are well described by
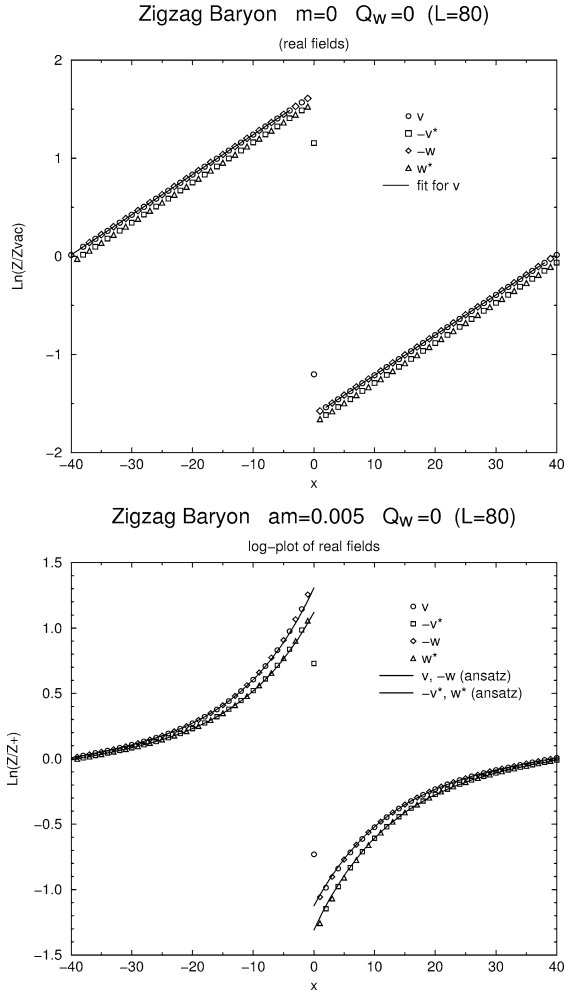
Fig. 12. Numerical zigzag baryon for the case with chiral symmetry (top) and without (bottom). We plot the (real) fields on a logarithmic scale. Top: a linear fit yields the slope $c_+ = 0.04$ and the field on the baryon $v(0) = 0.1735$, in excellent agreement with formulas (86). Bottom: we use the exponential ansatz of Section 7.2.1, with coefficients $\epsilon_\pm$ fitted over the domain $|x'| < 30$. The values $\epsilon_+ = 0.062$, $\epsilon_- = -0.053$ are in good agreement with the analytical theory.

$$v(x') = z_{\text{vac}} e^{c_+(x'+1)}, \qquad v^*(x') = z_{\text{vac}} e^{-c_+(x'-1)},$$
$$w(x'+1) = z_{\text{vac}} e^{-c_+(x'+2)}, \qquad w^*(x'+1) = z_{\text{vac}} e^{c_+ x'}, \tag{85}$$

where the value of the real coefficient c_+ is small (for a lattice of length $L = 80$, we found $c_+ \approx 0.04$). At all points $x \neq 0$, the fields are close to a "generalized homogeneous vacuum".

The coefficient c_+ can be analytically estimated by using the above ansatz for w, w^* at the position $x' = -1 + L/2$, and then enforcing Eq. (83). One obtains (to lowest order in

c_+) the transcendental equation

$$c_+ e^{c_+ L} = 1, \tag{86}$$

with approximate solution $c_+ \approx L^{-1} \ln L$. The field on the baryon then takes the value

$$v(0) = v^*(0) = \frac{3z_{\text{vac}}}{2} \sqrt{c_+}.$$

This configuration is very "distorted" compared to the original contour of integration. Indeed, the ratios v/v^* and w/w^* are of order L in the vicinity of the string. In the case $L = 80$, the above equations yield $c_+ = 0.04018$, $v(0) = 0.1736$, which are in excellent agreement with our numerical data.

7.2.1. Zigzag baryon—broken chiral symmetry

If chiral symmetry is broken by a non-vanishing quark mass, the deviations from z_+ evolve exponentially with x' away from the antipodal point $x' = 0$. More precisely, in some domain $|x'| \ll L/2$ the fields should follow the ansatz

$$\begin{pmatrix} \delta z(x') \\ \delta z^*(x') \end{pmatrix} \approx \begin{pmatrix} \epsilon_+ (-e^{\gamma_{\text{zig}}})^{x'} + \epsilon_- (-e^{-\gamma_{\text{zig}}})^{x'} \\ -\epsilon_+ e^{\kappa_{\text{zig}}} (-e^{\gamma_{\text{zig}}})^{x'} - \epsilon_- e^{-\kappa_{\text{zig}}} (-e^{-\gamma_{\text{zig}}})^{x'} \end{pmatrix}.$$

From the mirror symmetry (84), the coefficients $\epsilon_\pm$ are related by

$$\epsilon_- = -e^{\kappa_{\text{zig}}} \epsilon_+. \tag{87}$$

We numerically computed a solution with $L = 80$, $am = 0.005$ (see Fig. 12, bottom), for which this ansatz works well up to the string. Using this fact, it is possible to estimate the value of ϵ_+ (the last remaining parameter), as in the chiral case. The crudest approximation yields the equation

$$-\epsilon_+ \kappa_{\text{zig}} C \, e^{2C\epsilon_+} = 2, \quad \text{with} \quad C \overset{\text{def}}{=} \exp\{\gamma_{\text{zig}}(L/2 - 1)\}.$$

The solution of this equation in the case $L = 80$, $am = 0.005$ is $\epsilon_+ = 0.0614$. This configuration has a mass $M = 2.885 \, a^{-1}$ with respect to the homogeneous vacuum.

There also exist topologically non-trivial vacuum and baryon saddle-point configurations with the symmetry (84). For example, Fig. 13 shows the solution in the sector $Q_w = 1$ with quark mass $am = 0.005$ on a lattice of length $L = 160$. With respect to the corresponding vacuum configuration, this configuration has a mass $M = 3.18 \, a^{-1}$.

8. Concluding remarks

The "color-flavor transformation" introduced in [14,15] replaces an integral over the gauge group $U(N_c)$ by an integral over the "flavor" degrees of freedom. In the present paper we extended this transformation to the gauge group $SU(N_c)$.

The color-flavor transformation can be interpreted as a kind of duality, linking two different formulations of the theory. We believe that this duality transformation may be useful for treating realistic non-perturbative QCD. Here we have applied it to a simple model of two-dimensional lattice fermions. The non-Abelian theory we have treated is
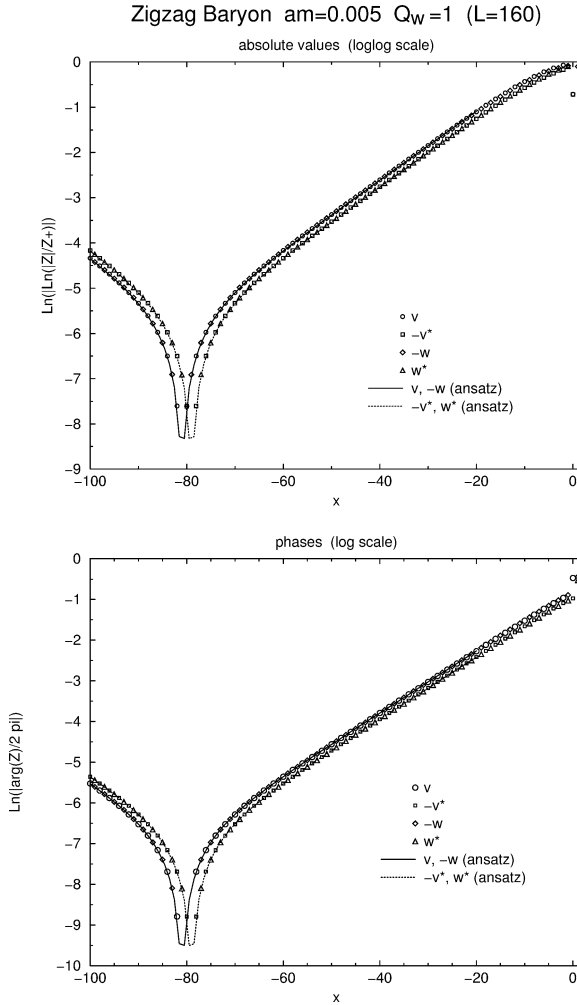
Fig. 13. Numerical zigzag baryon with winding number $Q_w = 1$ and broken chiral symmetry. We plot the real (top) and imaginary (bottom) parts of $\log(z/z_+)$ on a logarithmic scale, together with a fit by the ansatz (7.2.1) in the region $|x'| < 60$. The coefficients take the values $\epsilon_+ \approx (3.48 + i1.07) \times 10^{-3}$, $\epsilon_- \approx -(3.00 + i0.92) \times 10^{-3}$, and satisfy quite well the relation (87).

of course too far from realistic four-dimensional QCD for our results to be of direct phenomenological relevance.

The main approximation we made was to assume the strong-coupling limit for the lattice gauge fields. In this approximation gluons do not propagate, and the connection to asymptotic freedom at short distances is lost. An unphysical consequence is the absence of the U(1) chiral anomaly. Thus, the chiral symmetry group of our low-energy effective action is not $SU(N_f)$ but the larger group $U(N_f)$.

Among the gauge groups $\mathrm{SU}(N_c)$ the case $N_c = 2$ is special, as the vector and covector representations of $\mathrm{SU}(2)$ happen to be equivalent. Since these representations correspond to quarks and antiquarks, respectively, there is no physical distinction between baryons and mesons in that case. This symmetry between baryons and mesons is obscured in the present treatment which, by the use of a saddle-point approximation valid only for $N_c \gg 1$, is geared to the large-N_c limit. It can, however, be made manifest by identifying $\mathrm{SU}(2)$ with the compact symplectic gauge group $\mathrm{Sp}(2)$ and using the color-flavor transformation for the latter [15].

To extend the formalism to lattice QCD in four dimensions, we need to take into account the spin degrees of freedom and put the chiral fermions properly on the lattice. We hope to address these issues in a separate publication. Here we only note that a first step towards a more realistic color-flavor transformed theory of the strong interaction was described in [22,24], where we discuss the effect of spontaneous chiral symmetry breaking and estimate the numerical values of the chiral condensate, the pion decay constant and the mass of the pion.

Acknowledgements

Appendix A. Action of the color and flavor groups

Transformations $U \in \mathrm{GL}(N_c)$ of color space act on the one-fermion operators by

$$T_U f_{+a}^k T_U^{-1} = f_{+a}^j (U^{-1})^{kj}, \quad T_U f_{-a}^k T_U^{-1} = f_{-a}^j U^{jk},$$
$$T_U \bar{f}_{+a}^k T_U^{-1} = \bar{f}_{+a}^j U^{jk}, \qquad T_U \bar{f}_{-a}^k T_U^{-1} = \bar{f}_{-a}^j (U^{-1})^{kj}.$$

Transformations $\left(\begin{smallmatrix} A & B \\ C & D \end{smallmatrix} \right) \in \mathrm{GL}(2N_f)$ of flavor space can be decomposed in the way shown in Eq. (13), and the action of the various factors may be described separately. An element $\zeta = \left(\begin{smallmatrix} 1 & Z \\ 0 & 1 \end{smallmatrix} \right) = \exp\left(\begin{smallmatrix} 0 & Z \\ 0 & 0 \end{smallmatrix} \right)$ acts by

$$T_\zeta f_{+b}^k T_\zeta^{-1} = f_{+b}^k - \bar{f}_{-a}^k Z_{ba}, \quad T_\zeta f_{-b}^k T_\zeta^{-1} = f_{-b}^k + \bar{f}_{+a}^k Z_{ab},$$
$$T_\zeta \bar{f}_{+b}^k T_\zeta^{-1} = \bar{f}_{+b}^k, \qquad T_\zeta \bar{f}_{-b}^k T_\zeta^{-1} = \bar{f}_{-b}^k,$$

an element $\mathrm{diag}(A, D) = \left(\begin{smallmatrix} A & 0 \\ 0 & D \end{smallmatrix} \right) \in \mathrm{GL}(2N_f)$ by

$$T_{\mathrm{diag}(A,D)} f_{+b}^k T_{\mathrm{diag}(A,D)}^{-1} = f_{+a}^k (A^{-1})_{ba}, \quad T_{\mathrm{diag}(A,D)} f_{-b}^k T_{\mathrm{diag}(A,D)}^{-1} = f_{-a}^k D_{ab},$$
$$T_{\mathrm{diag}(A,D)} \bar{f}_{+b}^k T_{\mathrm{diag}(A,D)}^{-1} = \bar{f}_{+a}^k A_{ab}, \quad T_{\mathrm{diag}(A,D)} \bar{f}_{-b}^k T_{\mathrm{diag}(A,D)}^{-1} = \bar{f}_{-a}^k (D^{-1})_{ba},$$

and an element $\tilde{\zeta} = \left(\begin{smallmatrix} 1 & 0 \\ \tilde{Z} & 1 \end{smallmatrix} \right) \in \mathrm{GL}(2N_f)$ by

$$T_{\tilde{\zeta}} f^k_{+b} T^{-1}_{\tilde{\zeta}} = f^k_{+b}, \qquad\qquad T_{\tilde{\zeta}} f^k_{-b} T^{-1}_{\tilde{\zeta}} = f^k_{-b},$$
$$T_{\tilde{\zeta}} \bar{f}^k_{+b} T^{-1}_{\tilde{\zeta}} = \bar{f}^k_{+b} + f^k_{-a} \widetilde{Z}_{ab}, \quad T_{\tilde{\zeta}} \bar{f}^k_{-b} T^{-1}_{\tilde{\zeta}} = \bar{f}^k_{-b} - f^k_{+a} \widetilde{Z}_{ba}.$$

All these formulas are particular cases of the fermionic Fock-space representation of the Lie group $\mathrm{GL}(2N_f)$ expounded in Chapter 9 of [19].

Appendix B. Normalization constants

We are going to calculate the normalization constants $\alpha^{-1}_Q = \int_G dg \, |\langle B_Q | T_g | B_Q \rangle|^2$ introduced in Eq. (11)—for the values $Q = 1, 0, -1$. To that end, we employ the decomposition of the group $G = \mathrm{U}(2N_f)$ given by Eqs. (13) and (14). This yields

$$\left| \langle B_1 | T_g | B_1 \rangle \right|^2 = \frac{|(\sqrt{1 + ZZ^\dagger})_{1a} \mathcal{U}_{a1}|^{2N_c}}{\mathrm{Det}(1 + ZZ^\dagger)^{N_c}}$$

for $Q = 1$, and similar expressions for the other two cases. The first step now is to do the integral over $\mathcal{U} \in \mathrm{U}(N_f)$, which for $Q = \pm 1$ is effectively an integral over a $(2N_f - 1)$-dimensional sphere. Carrying it out by the method of Section 2.5, we get the preliminary expressions

$$\alpha^{-1}_0 = C_{N_f} \int_{\mathbb{C}^{N_f \times N_f}} \frac{dZ \, dZ^\dagger}{\mathrm{Det}(1 + ZZ^\dagger)^{2N_f + N_c}}, \tag{B.1}$$

$$\alpha^{-1}_1 = \alpha^{-1}_{-1} = C_{N_f} \frac{(N_f - 1)! N_c!}{(N_c + N_f - 1)!} \int_{\mathbb{C}^{N_f \times N_f}} \frac{[(1 + Z^\dagger Z)_{11}]^{N_c} dZ \, dZ^\dagger}{\mathrm{Det}(1 + ZZ^\dagger)^{2N_f + N_c}}, \tag{B.2}$$

where C_{N_f} is defined by

$$C^{-1}_{N_f} = \int_{\mathbb{C}^{N_f \times N_f}} \frac{dZ \, dZ^\dagger}{\mathrm{Det}(1 + ZZ^\dagger)^{2N_f}}. \tag{B.3}$$

For later convenience, we have made a change of integration variables $Z \leftrightarrow Z^\dagger$ in the numerator of the integral in (B.2).

In the second step we perform the integration over the $N_f \times N_f$ matrix Z using a recursion procedure similar to that in [25]. From here on we use the simplified notation $n = N_f$. The recursion consists in slicing the matrix Z into vertical vectors, step by step. We now detail the first step of the recursion. We decompose Z as $Z = (Z_{n,n-1}, z_1)$, where z_1 is a (column) n-vector, and $Z_{n,n-1}$ is a $n \times (n-1)$ matrix. We then have the expressions

$$ZZ^\dagger = Z_{n,n-1} Z^\dagger_{n,n-1} + z_1 z^\dagger_1, \qquad (Z^\dagger Z)_{11} = \left(Z^\dagger_{n,n-1} Z_{n,n-1} \right)_{11}.$$

Using the (positive definite) $n \times n$ matrix Γ_1 which is defined as the square root of

$$\Gamma^2_1 = 1 + Z_{n,n-1} Z^\dagger_{n,n-1},$$

we make a change of variables, from z_1 to $w_1 = \Gamma_1^{-1} z_1$. From $1 + ZZ^\dagger = \Gamma_1(1 + w_1 w_1^\dagger)\Gamma_1$, we get the relation

$$\mathrm{Det}\big(1 + ZZ^\dagger\big) = \big(1 + w_1^\dagger w_1\big) \mathrm{Det}\big(1 + Z_{n,n-1} Z_{n,n-1}^\dagger\big).$$

The change of variables from Z to $\{Z_{n,n-1}, w_1\}$ has the Jacobian $\mathrm{Det}(1 + Z_{n,n-1} Z_{n,n-1}^\dagger)$. Each of the integrals (B.1), (B.2), and (B.3) can now be written as the product of a $Z_{n,n-1}$–integral times a w_1-integral.

The former can in turn be expressed as the product of a $Z_{n,n-2}$-integral times a w_2-integral (with w_2 a n-vector), which can be decomposed in turn, and so on, until we reach, at the nth step, a $Z_{n,1}$-integral, i.e., an integral over the first column of the original matrix Z. We call this column vector w_n for reasons of homogeneity.

The successive Jacobians multiply to give the following integration measure:

$$dZ\,dZ^\dagger = dw_1^\dagger dw_1 \big(1 + w_2^\dagger w_2\big) dw_2^\dagger\, dw_2 \cdots \big(1 + w_n^\dagger w_n\big)^{n-1} dw_n\, dw_n^\dagger.$$

The integrands in (B.1)–(B.3) also have simple expressions in the new variables, due to the identities $(Z^\dagger Z)_{11} = w_n^\dagger w_n$ and

$$\mathrm{Det}\big(1 + ZZ^\dagger\big) = \big(1 + w_1^\dagger w_1\big)\big(1 + w_2^\dagger w_2\big) \cdots \big(1 + w_n^\dagger w_n\big).$$

The w_i-integrals to be performed are all of the type $(N \geqslant n)$

$$\int_{\mathbb{C}^n} \frac{dw^\dagger\, dw}{(1 + w^\dagger w)^{N+1}} = \pi^n \frac{(N-n)!}{N!}.$$

The resulting expressions for the normalization constants are

$$\alpha_0 = \frac{1}{C_{N_f} \pi^{N_f^2}} \frac{(2N_f + N_c - 1)! \cdots (N_f + N_c)!}{(N_c + N_f - 1)! \cdots N_c!}, \tag{B.4}$$

$$\alpha_1 = \alpha_{-1} = \frac{1}{C_{N_f} \pi^{N_f^2}} \frac{N_f (2N_f + N_c - 1)! \cdots (N_f + N_c + 1)!}{(N_c + N_f - 2)! \cdots N_c!}, \tag{B.5}$$

$$C_{N_f} = \frac{1}{\pi^{N_f^2}} \frac{(2N_f - 1)! \cdots N_f!}{(N_f - 1)! \cdots 0!}, \tag{B.6}$$

where we have reinstated $n = N_f$. The quantity entering into the baryon mass is the ratio

$$\frac{\alpha_1}{\alpha_0} = \frac{N_f}{N_f + N_c}. \tag{B.7}$$

Appendix C. Static baryon

In this appendix we prove the formula (37) for the action functional of the static baryon sector. We need to integrate polynomials in the quark fields along the worldline of the baryon (the baryon "string"), weighted by the same Gaussian as in the vacuum sector.

We start out using the short-hand notation $t\hat{0} \equiv 0 + t\hat{0}$ of Section 3.1.2 for sites and links on the string. The part of the integrand containing the quark fields situated on the string,

namely $\psi(t\hat{0})$, $\bar{\psi}(t\hat{0})$ for $t = 0, \ldots, T - 1$, then reads

$$\chi_1\left(\bar{\psi}(0), N\left(\frac{1}{2}\hat{0}\right)\psi(1\hat{0})\right)\chi_1\left(\bar{\psi}(1\hat{0}), N\left(\frac{3}{2}\hat{0}\right)\psi(2\hat{0})\right)$$

$$\cdots\chi_1\left(\bar{\psi}((T-1)\hat{0}), N\left(\left(T - \frac{1}{2}\right)\hat{0}\right)\psi(T\hat{0})\right)\exp-\left[\sum_{t=0}^{T-1}\bar{\psi}^i(t\hat{0})M(t\hat{0})\psi^i(t\hat{0})\right].$$

Isolating the terms with fermions at the site $n = t\hat{0}$, we are faced with the integral

$$\int d\bar{\psi}(n)\,d\psi(n)\,\chi_1\big(\bar{\psi}(n-\hat{0}), N(n-\hat{0}/2)\psi(n)\big)$$

$$\times\,\mathrm{e}^{-\bar{\psi}(n)M(n)\psi(n)}\chi_1\big(\bar{\psi}(n), N(n+\hat{0}/2)\psi(n+\hat{0})\big)$$

$$=\left(\alpha_1\frac{(N_f-1)!}{(N_c+N_f-1)!}\right)^2\int\prod_{i,a}d\bar{\psi}_a^i(n)\,d\psi_a^i(n)\mathrm{e}^{-\bar{\psi}_c^k(n)M_{cc'}(n)\psi_{c'}^k(n)}$$

$$\times\sum_{\sigma,\tau\in\mathfrak{S}_{N_c}}\mathrm{sgn}\,\sigma\,\mathrm{sgn}\,\tau\prod_i\bar{\psi}_a^i(n-\hat{0})N_{ab}(n-\hat{0}/2)\psi_b^{\sigma(i)}(n)$$

$$\times\prod_j\bar{\psi}_{a'}^j(n)N_{a'b'}(n+\hat{0}/2)\psi_{b'}^{\tau(j)}(n+\hat{0})$$

$$=\left(\alpha_1\frac{(N_f-1)!}{(N_c+N_f-1)!}\right)^2\sum_{\sigma,\tau\in\mathfrak{S}_{N_c}}\mathrm{sgn}(\sigma\tau)\prod_i\left[\bar{\psi}_{a_i}^{\sigma^{-1}(i)}(n-\hat{0})N_{a_ib_i}(n-\hat{0}/2)\right.$$

$$\times\left\{\int d\bar{\psi}^i(n)\,d\psi^i(n)\,\psi_{b_i}^i(n)\bar{\psi}_{a_i'}^i(n)\mathrm{e}^{-\bar{\psi}^i(n)M(n)\psi^i(n)}\right\}$$

$$\times\left.N_{a_i'b_i'}(n+\hat{0}/2)\psi_{b_i'}^{\tau(i)}(n+\hat{0})\right],$$

where the first equality sign uses the expression (21) for the function χ_1. Note that the integral between curly brackets involves only fermions of color i. The fermionic version of Wick's theorem yields for it the value $M_{b_ia_i'}^{-1}(n)\,\mathrm{Det}\,M(n)$, so after combining the permutations σ and τ, the above expression becomes

$$\alpha_1^2\frac{(N_f-1)!^2}{(N_c+N_f-1)!^2}N_c!\,\mathrm{Det}\,M(n)^{N_c}$$

$$\times\sum_{\rho\in\mathfrak{S}_{N_c}}\mathrm{sgn}\,\rho\prod_i\bar{\psi}_{a_i}^i(n-\hat{0})G_{a_ib_i'}(n-\hat{0}\to n+\hat{0})\psi_{b_i'}^{\rho(i)}(n+\hat{0})$$

$$=\alpha_1\,\mathrm{Det}\,M(n)^{N_c}\binom{N_c+N_f-1}{N_f-1}^{-1}\chi_1\big(\bar{\psi}(n-\hat{0}), G(n-\hat{0}\to n+\hat{0})\psi(n+\hat{0})\big),$$

with the "propagator" $G(n-\hat{0}\to n+\hat{0})\overset{\mathrm{def}}{=}N(n-\hat{0}/2)M(n)^{-1}N(n+\hat{0}/2)$.

Repeating the procedure, we successively integrate over the quark fields along the string, by which process the matrices N and M get organized into a single propagator. In the final integration step, we need to take into account the periodic boundary conditions for the

quark fields: $\psi(T\hat{0}) = \psi(0)$. The final integral over $\psi(0)$ then reads

$$\int d\bar{\psi}(0)\, d\psi(0)\, \chi_1\big(\bar{\psi}(0), G(0 \to T\hat{0})\psi(0)\big) e^{-\bar{\psi}(0)M(0)\psi(0)}.$$

We now use the following expression for the function χ_1:

$$\chi_1(\bar{\phi}, \phi) = \alpha_1 \frac{(N_f - 1)!}{(N_c + N_f - 1)!} \sum_{\{a_i\}} \sum_{\sigma \in \mathfrak{S}_{N_c}} \prod_{i=1}^{N_c} \bar{\phi}_{a_i}^i \phi_{a_{\sigma(i)}}^i,$$

which is easily obtained from Eq. (21) by interchanging the product over colors with the sum over flavors. Wick's theorem then yields for the $\psi(0)$-integral the result

$$\alpha_1 \frac{(N_f - 1)!}{(N_c + N_f - 1)!} \operatorname{Det} M(0)^{N_c} (-1)^{N_c} \sum_{\{a_i, b_i\}} \sum_{\sigma \in \mathfrak{S}_{N_c}} \prod_i G_{a_{\sigma(i)} b_i}(0 \to T\hat{0}) M_{b_i a_i}^{-1}(0).$$

The last matrix product may also be expressed in terms of the propagator G defined in Eq. (36), $\mathsf{G} = G(0 \to T\hat{0})M(0)^{-1}$.

What is the interpretation of the sign factor $(-1)^{N_c}$? To answer that question, recall that we evaluated the Grassmann field integral using *time-periodic* boundary conditions (instead of the conventional time-antiperiodic ones). In a d-dimensional quantum mechanical frame work with Hamiltonian H and inverse temperature β, this would mean that we are computing not the usual partition function but rather the *supertrace* $\operatorname{Tr}(-1)^{N_F} e^{-\beta H}$ with N_F the total fermion number. The overall sign factor $(-1)^{N_c}$ originates from that very fermion number, and is simply telling us that the baryon is a fermion (boson) if N_c is odd (respectively, even).

Let us take a closer look at the contributions from the sum over permutations $\sigma \in \mathfrak{S}_{N_c}$. Each permutation σ can be uniquely decomposed into a product of independent cycles. Denoting by $c_l(\sigma)$ the number of cycles of length l in this decomposition, the contribution from σ to the partition function can be written as

$$\sum_{\{a_i\}} \prod_{i=1}^{N_c} \mathsf{G}_{a_i a_{\sigma(i)}} = \prod_{l=1}^{N_c} (\operatorname{Tr} \mathsf{G}^l)^{c_l(\sigma)}.$$

The permutation group $\mathfrak{S}_{N_c}$ may be partitioned into disjoint classes with respect to conjugation (σ, σ' are said to be conjugate to each other iff there exists a permutation τ such that $\sigma' = \tau^{-1} \sigma \tau$). Two permutations σ and σ' are in the same conjugacy class iff they have the same cycle structure, i.e., $\forall l : c_l(\sigma) = c_l(\sigma')$. This allows to rewrite the sum over σ as a sum over the conjugacy classes $\hat{\sigma} \in \widetilde{\mathfrak{S}}_{N_c}$, taking into account the cardinality of each class, $\mathcal{N}(\hat{\sigma})$, given in Eq. (38). We then obtain the result (37).

References

[1] U.G. Meißner, Rep. Prog. Phys. 56 (1993) 903.
[2] T. Schafer, E.V. Shuryak, Rev. Mod. Phys. 70 (1998) 323.
[3] D. Diakonov, Chiral quark–soliton model, Lectures given at advanced summer school on nonperturbative quantum field physics, Peniscola, Spain, June 1997, hep-ph/9802298.

 [4] D.I. Diakonov, V.Yu. Petrov, Nucl. Phys. B 245 (1984) 259.
 [5] S. Weinberg, Phys. Rev. Lett. 18 (1967) 188;
     S. Weinberg, Phys. Rev. 166 (1968) 1568.
 [6] S. Myint, C. Rebbi, Nucl. Phys. B 421 (1994) 241.
 [7] K. Wilson, Phys. Rev. D 10 (1974) 2445.
 [8] M. Creutz, Quarks, Gluons and Lattices, Cambridge Univ. Press, Cambridge, 1983.
 [9] J. Gasser, H. Leutwyler, Ann. Phys. 158 (1984) 142;
     J. Gasser, H. Leutwyler, Nucl. Phys. B 250 (1985) 465.
[10] A.R. Levi, V. Lubicz, C. Rebbi, Phys. Rev. D 56 (1997) 1101.
[11] H. Kluberg-Stern et al., Nucl. Phys. B 190 (1981) 504.
[12] N. Kawamoto, J. Smit, Nucl. Phys. B 192 (1981) 100.
[13] A.B. Balantekin, Character expansions, Itzykson–Zuber integrals, and the QCD partition function, hep-th/0007161.
[14] M.R. Zirnbauer, J. Phys. A 29 (1996) 7113.
[15] M.R. Zirnbauer, The color-flavor transformation and a new approach to quantum chaotic maps, Proceedings of the XIIth international congress of mathematical physics, Brisbane, July 1997, chao-dyn/9810016.
[16] A. Altland, B.D. Simons, Nucl. Phys. B 562 (1999) 445.
[17] B. Schlittgen, T. Wettig, Nucl. Phys. B 632 (2002) 155.
[18] R. Howe, Remarks on classical invariant theory, Trans. Amer. Math. Soc. 313 (1989) 539.
[19] A. Perelomov, Generalized Coherent States and Their Applications, Springer-Verlag, Berlin, 1985.
[20] B.L. Ioffe, Nucl. Phys. B 188 (1981) 317.
[21] Chr.V. Christov et al., Prog. Part. Nucl. Phys. 37 (1996) 91.
[22] J. Budczies, Y. Shnir, Color-flavor transformation for the special unitary group and application to low energy QCD, in: M.N. Dubinin, V.I. Savrin (Eds.), Proceedings of 15th International Workshop on High Energy Physics and Quantum Field Theory, MSU, Moscow, 2001, p. 317, hep-lat/0101016.
[23] T. Nagao, S.M. Nishigaki, Phys. Rev. D 64 (2001) 014507, hep-lat/0012029.
[24] J. Budczies, Y. Shnir, AIP Conf. Proc. 508 (2000) 172.
[25] L.K. Hua, Harmonic Analysis of Functions of Several Variables in the Classical Domains, Science Press, 1959.